THERMODYNAMIC STUDIES ON COMPLEX DEOXIDATION OF LIQUID STEEL USING Mn, Si, Al AND Ca

by

G. BALACHANDRAN

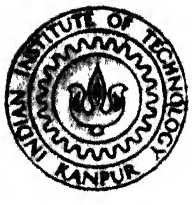

DEPARTMENT OF METALLURGICAL ENGINEERING
INDIAN INSTITUTE OF TECHNOLOGY KANPUR

AUGUST, 1986

THERMODYNAMIC STUDIES ON COMPLEX DEOXIDATION OF LIQUID STEEL USING Mn, Si, Al AND Ca

A Thesis Submitted

In Partial Fulfilment of the Requirements

for the Degree of

MASTER OF TECHNOLOGY

by

G. BALACHANDRAN

to the

DEPARTMENT OF METALLURGICAL ENGINEERING

INDIAN INSTITUTE OF TECHNOLOGY KANPUR

AUGUST, 1986

ME-1986-M-BAL-THE

To

Ponnatha

&

Kittamma

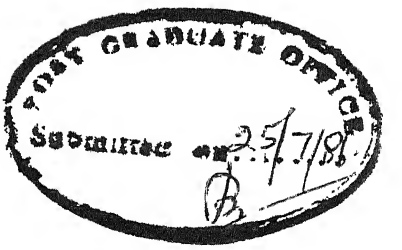

CERTIFICATE

Certified that this work on "Thermodynamic Studies on Complex Deoxidation of Liquid Steel Using Mn, Si, Al and Ca" has been carried out under our supervision and that it has not been submitted elsewhere for a degree.

A. Ghosh
Professor

Brahma Deo
Assistant Professor

Department of Metallurgical Engineering
Indian Institute of Technology
Kanpur-208016

ACKNOWLEDGEMENTS

I take this opportunity to express my sincere thanks to Dr. A. Ghosh and Dr. Brahma Deo for having involved me in the interesting field of Thermodynamics. It is a rewarding experience to have got an exposure to research work. Their efforts to get me literature and other necessary details from various quarters and their invaluable advices at various stages of the project requires special mention.

I wish to place on record the kind help rendered by B.T. Viswanath, Department of Mathematics in translating some of the literature. The company of Shri Awadesh Sharma and other lab mates had been a constant source of inspiration. I thank Shri R.N. Srivastava for typing this project report and Shri V.P. Gupta for drafting the figures.

- G. Balachandran.

CONTENTS

LIST OF TABLES

LIST OF FIGURES

LIST OF SYMBOLS USED IN THE THERMODYNAMIC MODELS AND FIGURES

K_i	Equilibrium constant of component i
a_i	Raoultian activity of component i
h_i	Henrian activity of component i
WMn	Weight percent manganese
WSi	Weight percent silicon
WAl	weight percent aluminium
WCa	Weight percent calcium
WO	Weight percent oxygen
WC	Weight percent carbon
e_i^j	interaction parameter of the interaction of component j over i
f_i	Henrian activity coefficient of component i
T	Temperature

ABSTRACT

Deoxidation of liquid steel is an important step in controlling the quality and grade of steel. The commonly used deoxidisers are Mn, Si, Al and Ca in the order of increasing deoxidising power. The combination of Mn-Si, Si-Ca, Ca-Al etc. are used to enhance the deoxidising power of simple deoxidisers The product of deoxidation may therefore be a simple or complex oxide mixture of MnO, SiO_2, Al_2O_3 and FeO. The formation of FeO is unavoidable in most cases. The steel maker is usually interested in obtaining low activities in the oxide phase and liquid deoxidation products.

In the present work, computer oriented thermodynamic models have been developed to study the deoxidation equilibria in various systems. Extensive literature survey has been carried out on activity-composition data for the binary and ternary slag systems involved. The role of FeO has been studied wherever possible.

The results of simple and complex deoxidation involving FeO as a component shows that the equilibrium concentration of the deoxidiser is significantly lowered by the formation of FeO-M_xO_y type product. The influence of temperature and the effect of presence of carbon in metal have been discussed.

The deoxidation involving Mn-Si, Ca-Si, Ca-Al and Ca-Mn have been studied with their respective oxides (M_xO_y-N_pO_q type) as the complex deoxidation products. From the

results obtained deoxidation powers of the above systems has been established. The role of FeO in the above systems has been studied. The equilibrium contents of the deoxidisers and oxygen dissolved in metal could be found from the slag composition of the ternary slag systems ($FeO-MnO-SiO_2$, $FeO-CaO-SiO_2$ and FeO-CaO-MnO) using the thermodynamic models developed.

Chapter 1

GENERAL CONSIDERATIONS IN THE DEOXIDATION OF STEEL

1.1 Introduction

The liquid steel at the end of refining usually contains 0.05 to 0.1 percent of dissolved oxygen. It is necessary to control the amount of dissolved oxygen as during solidification of the ingots or steel castings oxygen and carbon in solution may react to give carbon monoxide resulting in the formation of undesirable blowholes. Further, on cooling the steel the oxygen comes out of solution as oxides of iron, manganese, aluminium, silicon etc., which may be entrapped in solid steel as inclusions. These inclusions impair the hot and cold workability of the steel and also its mechanical properties.[1]

The solubility of oxygen in liquid iron[2], at the melting point, is about 0.16% and it increases with temperature according to the equation,

$$\log(\%O) = -\frac{6320}{TEMP} + 2.734$$

In solid iron, the solubility of oxygen tends to be negligible with increasing purity. Therefore, at the time of tapping, the excess oxygen content of the liquid steel must be reduced to the desired level to produce the required grade of steel (rimming, semikilled or fully killed). The removal of oxygen may be accomplished by adding to liquid steel those elements which have higher affinity for oxygen than

iron. This process is known as precipitation deoxidation. The dissolved oxygen in steel may diffuse to a suitable slag on the steel surface. This is known as diffusion deoxidation.

The reaction of deoxidising elements with oxygen may occur at constant temperature and give primary deoxidation products which have greater opportunity to escape from the steel melt. Deoxidation reactions may also occur during cooling of both the liquid and solid steel by virtue of segregation of alloying elements, decreasing temperature and decreasing solubility of oxygen. This is called as secondary deoxidation. The products of reaction may be entrapped in steel as inclusions. The influence of these inclusions on steel properties are discussed by Kiessling[3] and Pickering.[4]

1.2 Effect of Carbon on Deoxidation[5]

Oxygen solubility in γ-iron is around 0.003%. If carbon content is not greater than 0.1% most of the excess oxygen combines with C to form CO. Some of the CO escapes as gas while some entrapped in metal compensates solidification shrinkage. The gas evolution is small when carbon content is greater than 0.1%, till about 2% carbon after which the solubility of oxygen in steel approaches that in solid state. In the steel making furnaces the actual oxygen content of the metal is greater than that in equilibrium with carbon. It is found that the equilibrium is approached more closely during the transfer of metal from furnace to moulds. This may be due to:

a) the reduction of ferrostatic pressure and increased turbulence promoting bubble formation as metal flows to ladle.

b) the fluxing action of the bubbles of steam formed by moisture in the casting pit refractories which rise through metal and absorb CO in transit.

The addition of other deoxidisers suppresses the carbon boil. The deoxidation reactions continue at the interface after the reactions in the bulk metal have ceased. Hence, the residual concentration of the deoxidising elements in the metal are progressively lowered and the oxygen content increases which may recommence the carbon boil. The amount of oxygen transferred across the interface per unit time depends on total area of interface per unit mass of steel. Bagaria[6] has discussed the equilibrium between carbon and oxygen in steel.

1.3 Scope of the Present Work

In the present work, the equilibrium content of oxygen corresponding to the equilibrium contents of deoxidisers after deoxidation has been evaluated through various calculation models. The systems for which the investigation is carried out are Al, Si, Mn and Ca as single deoxidisers and Si-Mn, Ca-Si, Ca-Mn and Ca-Al as double deoxidisers. The following are the assumptions involved:

a) Only precipitation deoxidation is considered.

b) The equilibrium is reached and the kinetic aspects are not considered.

c) The complex slag formed is a homogeneous mixture of the component oxides involved.

d) The calculation is restricted to the liquid regions of the slag systems, that is, the product slag is liquid.

e) As deoxidation progresses there is no transfer of oxygen to the metal through the slag.

f) The simultaneous deoxidation by carbon has not been considered.

g) There is no other impurity other than the deoxidisers, carbon and oxygen.

h) Intermediate compound formation of the slag products are not considered.

i) There exists the formation of FeO which influences the equilibria.

1.4 Role of Wustite (Fe_xO)

Ferrous oxide is a non-stoichiometric compound and its composition is stated as Fe_xO, where x ranges from 0.97 to 1.0. The Fe-O phase diagram shows that values of x in equilibrium with liquid iron is 0.97 at 1500°C and 0.98 at 1600°C. The value of x is also a function of oxygen potential. In a complex slag, oxygen potential decreases with decrease in the activity of FeO. Since the variation in x is small, the equilibrium oxygen content is affected only marginally. In the present work, a constant value of $x = 1$, has been used. The errors arising due to this assumption are much less than the uncertainties in the reported values of activity of FeO itself.

1.5 Compilation of Thermodynamic Data

The equilibrium constants used in the present work are those compiled by Ghosh et al[7] (Table 1). The interaction parameters values are taken from Sigworth and Elliott[8] (Table 2), except for the values of e_O^{Ca} and e_{Ca}^{O}, which were not reported by them. The values of e_O^{Ca} and e_{Ca}^{O} suggested by various authors are compiled in Table 3, which show large variation.

Sponseller and Flinn[9] obtained $e_O^{Ca} = -1.4$ and $e_{Ca}^{O} = -3.6$. Kobyashi et al[10] have reported values of $e_O^{Ca} = -1330$ and $e_{Ca}^{O} = -535$. Faulring and Ramalingam[11] in their study on calcium based complex deoxidation reported that the use of high interaction parameter values of Kobyashi gave weight percent oxygen values that were significantly greater than the henrian activity of oxygen. Although they recommended the use of $e_O^{Ca} = -1.4$ and $e_{Ca}^{O} = -3.6$, they avoided the calculation of weight percentages and have expressed all their results in henrian activities. Later work by Gustafsson et al[12] recommend $e_O^{Ca} = -62.0$ for calcium contents between 20 and 170 ppm. They suggested variation of interaction parameter values with concentration of calcium.

In the present work the recommended values of Sponseller and Flinn[9] have been used.

Table 1

VALUES OF EQUILIBRIUM CONSTANTS FOR $x\,\underline{M} + y\,\underline{O} = M_xO_y$ TYPE REACTIONS

Element	Assumed deoxidation product	$\log_{10} K_M$
Fe	FeO(s)	$-\frac{6320}{TEMP} + 2.734$
Mn	MnO(s)	$-\frac{11070}{TEMP} + 4.526$
Si	SiO_2(s)	$-\frac{27893}{TEMP} + 10.27$
Al	Al_2O_3(s)	$-\frac{58473}{TEMP} + 17.74$
Ca	CaO(s)	$-\frac{32903}{TEMP} + 7.56$

Table 2

VALUES OF INTERACTION PARAMETERS

i \ j	Mn	Si	Al	Ca	O	C
Mn	-0.0029	0.065	-	-	-0.1	-0.108
Si	0.002	0.11	0.058	-0.067	-0.23	0.18
Al	0.0065	0.0056	0.045	-0.047	-6.6	0.091
Ca	-	-0.097	-0.072	-0.002	*	-0.34
O	-0.021	-0.131	-3.9	*	-0.2	-0.45

* Refer Table 3.

Table 3

VALUES OF Ca-O INTERACTION PARAMETERS REPORTED BY VARIOUS WORKERS

S.No.	e_O^{Ca}	e_{Ca}^{O}	Reference
1	-1.4	-3.6	Sponseller and Flinn[9]
2	-535.0	-1330.0	Kobyashi et al[10]
3	-24.75	-62.0	Gustaffson and Mellberg[12]
4	-150.0	-375.75	" "

Table 4

ACTIVITY-COMPOSITION DATA FOR $FeO-SiO_2$ SYSTEM AT 1350°C

S.No.	X_{SiO_2}	a_{FeO}	a_{SiO_2}
1	0.267	0.420	0.920
2	0.235	0.473	0.773
3	0.211	0.545	0.640
4	0.181	0.643	0.428
5	0.143	0.740	0.294
6	0.111	0.845	0.185
7	0.078	0.908	0.131
8	0.060	0.933	0.108
9	0.038	0.948	0.091

Chapter 2

DEOXIDATION EQUILIBRIA INVOLVING $FeO-M_xO_y$ (M = Mn, Si, Al, Ca) TYPE SLAGS

2.1 Introduction

In this chapter, thermodynamic calculation models have been developed to study the deoxidation equilibria between the deoxidants and oxygen in steel when complex slag of the type $FeO-M_xO_y$ (M = Mn, Si, Al, Ca) forms. The results obtained are compared with that of simple deoxidation giving the respective oxides as the deoxidation product. The calculation models in the present chapter require the slag activity data for the slag systems $FeO-M_xO_y$ and hence a thorough literature survey was carried out.

2.2 Choice of Activity Data

Depending upon the oxygen content of liquid steel, the deoxidation by single deoxidisers may result in complex slags $FeO-M_xO_y$ of varying composition. It is therefore necessary to examine the activity data available for $FeO-M_xO_y$ system.

2.2.1 System FeO-MnO

The system FeO-MnO is generally accepted as an ideal system and the same is assumed in the present work. There are very few reported variation from ideality. Fischer and Fleischer[13] determined the activity of MnO using MnO crucible. The results showed a non-ideal behaviour. Experimental

results by Fischer and Bardenheuer[14] were found to be scattered between the activity data of the previous work and ideal behaviour. Schwerdtfeger and Muan[15] reported that activities of Fe_tO and MnO exhibit positive deviation from Raoult's law when solid solution is formed. Turkdogan[16] has performed deoxidation equilibria calculations on manganese assuming ideal behaviour of FeO-MnO.

2.2.2 System $FeO-SiO_2$

This system exhibits a marked negative deviation from ideality. Schuhuman and Ensio[17] have obtained activity of FeO in their experimental study with pure FeO (liquid) in equilibrium with γ-iron as the standard state. They observed that the activity of FeO is not a function of temperature. Michal and Schuhuman[18] in their study with silica saturated iron silicate slags were also able to calculate activity of FeO. Turkdogan and Pearson[19] reviewed the work of Schuhuman and Ensio and suggested that activity of FeO depended upon the temperature and that beyond 0.75 N_{FeO}, $\gamma_{FeO} > 1$ could be doubted. They recalculated the activity of FeO in slag by dividing the equilibrium oxygen content of liquid iron with oxygen content of iron in contact with wustite at the same temperature. They suggested that as temperature increases the deviation from Raoult's law decreases. The silica activity calculated showed positive deviation.

Bodsworth[20] equilibrated H_2/steam mixtures and molten slags in solid iron crucibles and found that activity of FeO is not a function of temperature and that it exhibits

negative deviation from ideality throughout the concentration range. The activity of FeO is closer to that recorded for activity of MnO in binary melts. However, Bodsworth[5] suggests that $FeO-SiO_2$ system behaves ideally above 1600°C temperature. Elliott[21] supported the conclusion drawn by Turkdogan and Pearson. Turkdogan recalculated the activity of FeO at 1600°C by using the data of Schuhuman and Ensio by a theoretical approach. The standard state employed was liquid iron oxide in equilibrium with pure liquid iron and pure liquid silica. The dependence of activity of FeO on temperature was reemphasised. Banya et al[22] in their study with $H_2/H_2O/Ar$ gas mixture on equilibration with $FeO-SiO_2$ slags at 1400°C observed that the temperature dependence of activity of FeO is not significant. They further found that log γ_{FeO} is inversely proportional to temperature and using this dependence obtained data for activity FeO at 1600°C. In the present work the data of Schuhuman and Ensio,[17] at 1350°C has been used because of the reliability of their results. The data is compiled in Table 4.

2.2.3 System $FeO-Al_2O_3$

Very limited data are available on the variation of activity of FeO with composition due to the small region in which the liquid deoxidation products are formed. Banya et al[22] in their study of equilibration of $H_2/H_2O/Ar$ gas mixture with $FeO-Al_2O_3$ slag obtained the activity of FeO. It was observed that the activity of FeO exhibited negative deviation from Raoult's law. They compared their results with

Table 5

ACTIVITY-COMPOSITION DATA FOR $FeO-Al_2O_3$ SYSTEM AT 1400°C

S.No.	$X_{Al_2O_3}$	a_{FeO}	$a_{Al_2O_3}$
1	0.080	0.889	0.0195
2	0.085	0.891	0.0187
3	0.070	0.895	0.0168
4	0.090	0.897	0.0145
5	0.095	0.906	0.0145
6	0.100	0.920	0.0146
7	0.060	0.909	0.0140
8	0.075	0.891	0.0111
9	0.065	0.901	0.0111
10	0.055	0.919	0.0104
11	0.050	0.929	0.0851
12	0.040	0.951	0.0793
13	0.045	0.940	0.0699
14	0.035	0.962	0.0452
15	0.030	0.973	0.0221
16	0.025	0.982	0.0165
17	0.020	0.989	0.0134
18	0.015	0.995	0.0092
19	0.005	0.999	0.0074
20	0.010	0.998	0.0065

Maruhashi at 1560°C and found a large variation. In the present work, the results of Banya[22] has been used since the results of Maruhashi are not available for critical assessment. The data is compiled in Table 5.

2.2.4 System FeO-CaO

This system exhibits negative deviation from ideality. Elliott[21] estimated the activity of FeO as a function of mole fraction by a theoretical approach assuming that there was no intermediate compound formation. On extrapolating Taylor and Chipman's data over the entire concentration range they found negative deviation from ideality for the activity curves of FeO and CaO. The standard state used was lime saturated slag. Banya et al[22] equilibrated $H_2/H_2O/Ar$ gas mixture with FeO-CaO slags and obtained results in close agreement with those of Chipman. Their experiments were free from crucible contamination. Iwase et al[23] employed solid electrolyte to find the activity of FeO in FeO-CaO slag system in equilibrium with liquid iron. Their results generally agreed with those of Banya et al, but for a slight increase. In the present work the data from Iwase et al[23] have been used because there is no crucible contamination in their work and the inaccuracies due to chemical analysis were much less. The data is compiled in Table 6.

2.3 Regions of Phase Diagram Considered for Thermodynamic Calculation of FeO-M_xO_y Systems

The phase diagrams of the various FeO-M_xO_y systems are given in Figure 1 to Figure 4. The thermodynamic

Table 6

ACTIVITY-COMPOSITION DATA FOR FeO-CaO SYSTEM AT 1400°C

S.No.	X_{CaO}	a_{FeO}	a_{CaO}
1	0.00	1.000	0.00
2	0.05	0.965	0.05
3	0.10	0.925	0.11
4	0.15	0.875	0.20
5	0.20	0.810	0.32
6	0.25	0.740	0.45
7	0.30	0.655	0.61
8	0.35	0.555	0.83
9	0.36	0.525	0.90
10	0.40	0.525	0.90

Table 7

LIQUID RANGE IN $FeO-M_xO_y$ SYSTEMS

No.	System	Temperature °C	Liquid range in wt.pct. M_xO_y From	To	Figure
1	FeO-MnO	1400	0.0	7	1
		1500	0.0	24	
		1600	0.0	40	
2	$FeO-SiO_2$	1350	5.0	38	2
		1400	0.0	40	
		1500	0.0	43	
3	$FeO-Al_2O_3$	1400	0.0	8	3
4	FeO-CaO	1400	0.0	33	4

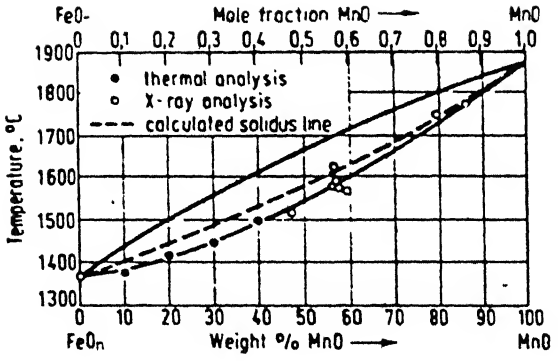

Fig. 1. Phase diagram for system FeO–MnO

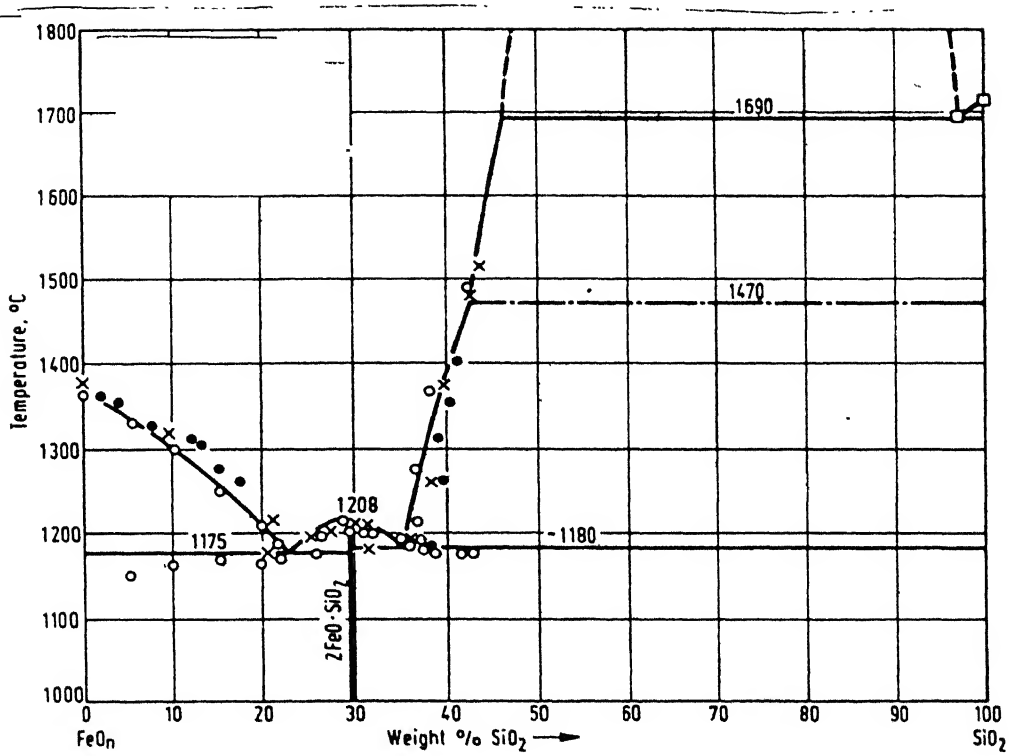

Fig. 2. Phase diagram for system FeO-SiO_2.

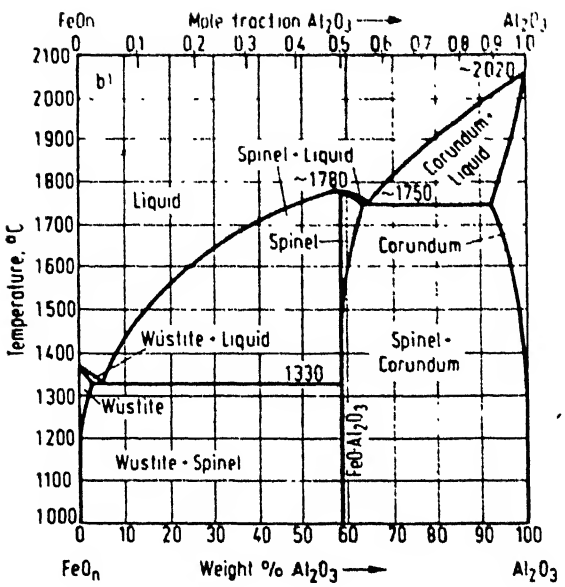

Fig. 3. Phase diagram for system $FeO-Al_2O_3$.

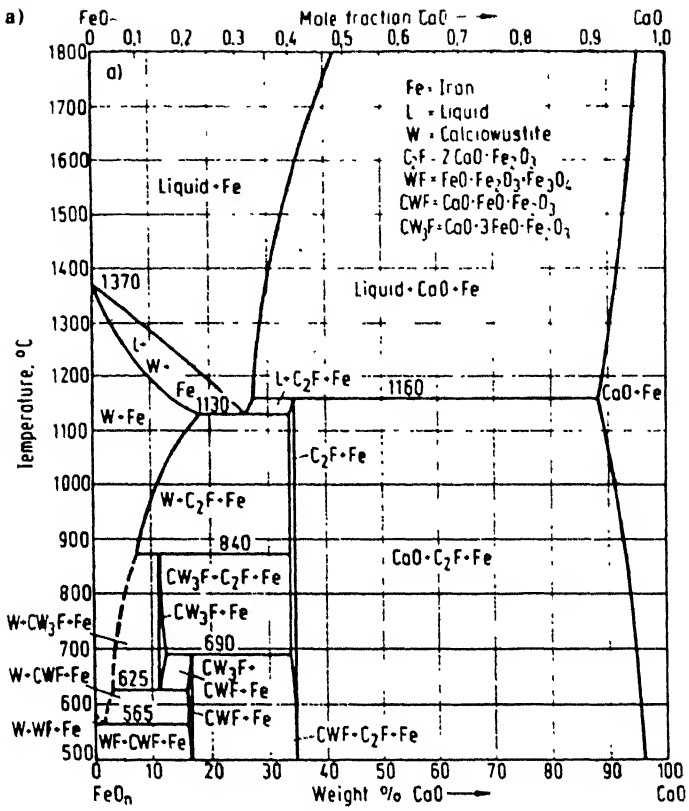

Fig. 4. Phase diagram for system FeO-CaO.

calculation are restricted to the regions where the deoxidation products, $FeO-M_xO_y$ are in liquid state. The slag composition range used for the particular temperature at which the analysis has been carried out for different systems has been compiled in Table 7.

2.4 Thermodynamic Models

2.4.1 Thermodynamic model for deoxidation by manganese

The basic reactions taking place are

$$Fe + \underline{O} = FeO(s) \qquad (1.1)$$

$$\underline{Mn} + \underline{O} = MnO(s) \qquad (1.2)$$

The equilibrium constants for the above reactions may be written as,

$$K_{Fe} = \frac{a_{FeO}}{h_O \; a_{Fe}}$$

Since iron is the solvent $a_{Fe} \simeq 1$

$$K_{Fe} = \frac{a_{FeO}}{h_O} \qquad (1.3)$$

and

$$K_{Mn} = \frac{a_{MnO}}{h_{Mn} \; h_O} \qquad (1.4)$$

The equation for K_{Fe} and K_{Mn} as functions of temperature are given in Table 1.

Since the FeO-MnO slag behaves ideally,

$$a_{FeO} = X_{FeO}$$

and

$$a_{MnO} = X_{MnO} \qquad (1.5)$$

From (1.1) to (1.5)

$$K_{Mn} = \left(\frac{X_{MnO}}{X_{FeO}}\right) \frac{K_{Fe}}{n_{Mn}} \qquad (1.6)$$

It is known that

$$X_{FeO} + X_{MnO} = 1 \qquad (1.7)$$

From (1.6) and (1.7),

$$X_{MnO} = \frac{K_{Mn} h_{Mn}}{K_{Fe} + K_{Mn} h_{Mn}} \qquad (1.8)$$

From (1.4), (1.5) and (1.8) substituting for X_{MnO},

$$h_O = \frac{1}{(K_{Fe} + K_{Mn} n_{Mn})} \qquad (1.9)$$

$$h_{Mn} = f_{Mn}\ W_{Mn}.$$

$$h_O = f_O\ W_O \qquad (1.10)$$

where,

$$f_{Mn} = 10^{\left(e_{Mn}^{Mn} \times W_{Mn} + e_{Mn}^{C} \times W_C + e_{Mn}^{O} \times W_O \right)} \qquad (1.11)$$

$$f_O = 10^{\left(e_O^{Mn} \times W_{Mn} + e_O^{C} \times W_C + e_O^{O} \times W_O \right)} \qquad (1.12)$$

$$W_O = \frac{1}{f_O (K_{Fe} + K_{Mn} h_{Mn})} \qquad (1.13)$$

For fixed values of temperature, W_C, W_{Mn} and using equations (1.10) to (1.13) the W_O values could be calculated. During the initial stages of calculation ($e_{Mn}^{O} \times W_O$) and ($e_O^{O} \times W_O$) terms are assumed zero. But after calculation of W_O by equation (1.13) the values are iterated back to

refine f_{Mn} and f_O till the successive value of WO converged with less than 0.5% error.

2.4.2 Thermodynamic models for deoxidation by silicon

Two thermodynamic models were developed for this system. Model 1 employs the same procedure of calculation as adopted by Bagaria[6]. Model 2 is an improvement over model 1.

Model 1

The basic reactions taking place are,

$$Fe + \underline{O} = FeO(s) \quad (2.1)$$

$$\underline{Si} + 2\underline{O} = SiO_2(s) \quad (2.2)$$

The equilibrium constants for the above reactions may be given as

$$K_{Fe} = \frac{a_{FeO}}{h_O \; a_{Fe}}$$

Since iron is the solvent $a_{Fe} \simeq 1$.

$$K_{Fe} = \frac{a_{FeO}}{h_O} \quad (2.3)$$

$$K_{Si} = \frac{a_{SiO_2}}{h_{Si} h_O^2} \quad (2.4)$$

The equations for K_{Fe} and K_{Si} as functions of temperatures are given in Table 1.

The slag activity data for the system $FeO-SiO_2$ is compiled in Table 4. For any fixed temperature between 1350°C and 1550°C, and for a given slag composition using

the activity of FeO (a_{FeO}) in equation (2.3) the h_O value was calculated. Using the corresponding value of activity of SiO_2 (a_{SiO_2}) in equation (2.4), h_{Si} was calculated. Now,

$$\log h_{Si} = \log WSi + e_{Si}^{Si} \times WSi + e_{Si}^{C} \times WC + e_{Si}^{O} \times WO \quad (2.5)$$

$$\log h_O = \log WO + e_O^{Si} \times WSi + e_O^{C} \times WC + e_O^{O} \times WO \quad (2.6)$$

For a fixed WC, it is possible to solve equations (2.5) and (2.6) for WSi and WO simultaneously using Newton-Raphson's technique in a matrix formulation using the procedure adopted by Bagaria[6].

Model 2

From the activity-composition data for $FeO-SiO_2$ system, Table 4, fifth order polynomial regression equations were obtained between the following quantities,

$$\log\left(\frac{a_{FeO}^2}{a_{SiO_2}}\right) \quad \text{Versus} \quad \log X_{SiO_2}$$

$$\log\left(\frac{a_{FeO}^2}{a_{SiO_2}}\right) \quad \text{Versus} \quad \log a_{SiO_2}$$

$$\log\left(\frac{a_{FeO}^2}{a_{SiO_2}}\right) \quad \text{Versus} \quad \log a_{FeO}$$

The regression equations fitted well with the actual data with error less than 1%.

From equations (2.3) and (2.4)

$$\frac{a_{FeO}^2}{a_{SiO_2}} = \left(\frac{K_{Fe}^2}{K_{Si}}\right) \frac{1}{h_{Si}} \quad (2.7)$$

$$h_{Si} = WSi \times f_{Si} \tag{2.8}$$

Further,

$$f_{Si} = 10^{(e_{Si}^{Si} \times WSi + e_{Si}^{C} \times WC + e_{Si}^{O} \times WO)} \tag{2.9}$$

$$f_{O} = 10^{(e_{O}^{Si} \times WSi + e_{O}^{C} \times WC + e_{O}^{O} \times WO)} \tag{2.10}$$

For a given value of temperature (between 1350°C and 1550°C), WC and WSi, f_{Si} and f_O can be calculated using equations (2.9) and (2.10). Initially the terms $(e_{Si}^{O} \times WO)$ and $(e_{O}^{O} \times WO)$ are assumed to be zero. The h_{Si} can be calculated using equation (2.8). The values of K_{Fe}, K_{Si} and h_{Si} in equation (2.7) gives (a_{FeO}^2/a_{SiO_2}). Corresponding to the $\log(a_{FeO}^2/a_{SiO_2})$, the values of $\log(X_{SiO_2})$, $\log(a_{SiO_2})$ and $\log(a_{FeO})$ can be found using the regression equations. From this a_{FeO}, a_{SiO_2} and X_{SiO_2} are found.

Considering the equations (2.2) and (2.4)

$$h_O^2 = \frac{a_{SiO_2}}{K_{Si}\ h_{Si}} \tag{2.4}$$

Since

$$h_O = WO \times f_O \tag{2.11}$$

From equations (2.4) and (2.11)

$$WO = \left(\frac{a_{SiO_2}}{K_{Si}\ h_{Si}\ f_O^2}\right)^{1/2} \tag{2.12}$$

The WO obtained from equation (2.12) is iterated back to refine f_O and f_{Si} till two consecutive values of WO agree with less than 0.5% error.

2.4.3 Thermodynamic models for deoxidation by aluminium

The two thermodynamic models developed for $FeO-SiO_2$ were applied here on the same lines to the $FeO-Al_2O_3$ system.

Model 1

The basic reactions are

$$Fe + \underline{O} = FeO(s) \qquad (3.1)$$

$$2\underline{Al} + 3\underline{O} = Al_2O_3(s) \qquad (3.2)$$

The equilibrium constants of the above reactions may be given as

$$K_{Fe} = \frac{a_{FeO}}{h_O \; a_{Fe}}$$

Since iron is the solvent $a_{Fe} \simeq 1$

$$K_{Fe} = \frac{a_{FeO}}{h_O} \qquad (3.3)$$

$$K_{Al} = \frac{a_{Al_2O_3}}{h_{Al}^2 \; h_O^3} \qquad (3.4)$$

The K_{Fe} and K_{Al} are given as a function of temperature in Table 1. The slag activity data for $FeO-Al_2O_3$ system is given in Table 5. For the reported temperature of slag activity data and for a fixed slag composition using the activity value of FeO in equation (3.3), the h_O value can be found. From the corresponding activity of Al_2O_3 and equation (3.4), the h_{Al} value can be found. Now

$$\log h_{Al} = \log WAl + e_{Al}^{Al} \times WAl + e_{Al}^{C} \times WC + e_{Al}^{O} \times WO \qquad (3.5)$$

$$\log h_O = \log WO + e_O^{Al} \times WAl + e_O^{C} \times WC + e_O^{O} \times WO \qquad (3.6)$$

For a fixed value of WC, it is possible to solve equations (3.5) and (3.6) for WAl and WO simultaneously using Newton-Raphson's technique as discussed earlier in Section 2.4.2, Model 1.

Model 2

From the activity composition data for FeO-Al_2O_3 system, Table 5, fifth order polynomial regression equations were obtained between the following quantities,

$$\log\left(\frac{a_{FeO}^3}{a_{Al_2O_3}}\right) \quad \text{Versus} \quad \log X_{Al_2O_3}$$

$$\log\left(\frac{a_{FeO}^3}{a_{Al_2O_3}}\right) \quad \text{Versus} \quad \log a_{FeO}$$

$$\log\left(\frac{a_{FeO}^3}{a_{Al_2O_3}}\right) \quad \text{Versus} \quad \log a_{Al_2O_3}$$

The regression equations fitted well with actual data with error less than 1%.

From equations (3.3) and (3.4)

$$\frac{a_{FeO}^3}{a_{Al_2O_3}} = \left(\frac{K_{Fe}^3}{K_{Al}}\right) \frac{1}{h_{Al}^2} \qquad (3.7)$$

$$h_{Al} = WAl \times f_{Al} \qquad (3.8)$$

Further,

$$(e_{Al}^{Al} \times WAl + e_{Al}^{C} \times WC + e_{Al}^{O} \times WO)$$

$$f_O = 10^{(e_O^{Al} \times WAl + e_O^{C} \times WC + e_O^{O} \times WO)} \qquad (3.10)$$

For the temperature reported in the slag activity data and an initial value of WC and WAl, the value of f_{Al} and f_O are calculated using equations (3.9) and (3.10). Initially the terms $(e_{Al}^{O} \times WO)$ and $(e_O^{O} \times WO)$ are assumed to be zero. The h_{Al} is calculated using equation (3.8). The values of K_{Fe}, K_{Al} and h_{Al} in equation (3.7) gives $(a_{FeO}^3/a_{Al_2O_3})$. Corresponding to the $\log(a_{FeO}^3/a_{Al_2O_3})$ using the regression equations $X_{Al_2O_3}$, a_{FeO} and $a_{Al_2O_3}$ can be found.

Considering equations (3.2) and (3.4)

$$h_O^3 = \frac{a_{Al_2O_3}}{K_{Al}\, h_{Al}^2} \qquad (3.4)$$

It is known that

$$h_O = WO \times f_O \qquad (3.11)$$

From equations (3.4) and (3.11),

$$WO = \left(\frac{a_{Al_2O_3}}{K_{Al}\, h_{Al}^2\, f_O^3}\right)^{1/3} \qquad (3.12)$$

The WO obtained from equation (3.12) is iterated back to refine f_O and f_{Al} till two consecutive values of WO agree with less than 1% error.

2.4.4 Thermodynamic models for deoxidation by calcium

The two thermodynamic models developed for the FeO-SiO_2 and FeO-Al_2O_3 systems were applied here on the same lines to the FeO-CaO system.

Model 1

The basic reactions taking place are,

$$Fe + \underline{O} = FeO(s) \quad (4.1)$$

$$\underline{Ca} + \underline{O} = CaO(s) \quad (4.2)$$

The equilibrium constant of the above reactions may be given as,

$$K_{Fe} = \frac{a_{FeO}}{h_O \; a_{Fe}}$$

Since iron is the solvent $a_{Fe} \simeq 1$

$$K_{Fe} = \frac{a_{FeO}}{h_O} \quad (4.3)$$

$$K_{Ca} = \frac{a_{CaO}}{h_{Ca} \; h_O} \quad (4.4)$$

The K_{Fe} and K_{Ca} are given as functions of temperature in Table 1. The slag activity data for FeO-CaO system is given in Table 6. For the temperature reported in the slag activity data and for a fixed slag composition, using the activity value of FeO in (4.3) the h_O value can be found. From the corresponding value of activity of CaO and equation (4.4) the h_{Ca} value can be found. Now

$$\log h_{Ca} = \log WCa + e_{Ca}^{Ca} \times WCa + e_{Ca}^{C} \times WC + e_{Ca}^{O} \times WO \quad (4.5)$$

$$\log h_O = \log WO + e_O^{Ca} \times WCa + e_O^{C} \times WC + e_O^{O} \times WO \quad (4.6)$$

For a fixed value of WC, it is possible to solve equations (4.5) and (4.6) for WCa and WO simultaneously using Newton-Raphson's technique as discussed in Sections 2.4.2 and 2.4.3,

Model 1

Model 2

From the activity composition data of FeO-CaO system Table 6, seventh order polynomial regression equations were obtained between the following quantities

$$\log\left(\frac{a_{FeO}}{a_{CaO}}\right) \quad \text{Versus} \quad \log X_{CaO}$$

$$\log\left(\frac{a_{FeO}}{a_{CaO}}\right) \quad \text{Versus} \quad \log a_{CaO}$$

$$\log\left(\frac{a_{FeO}}{a_{CaO}}\right) \quad \text{Versus} \quad \log a_{FeO}$$

The regression equations fitted well with the actual data with error less than 1%.

From equations (4.3) and (4.4)

$$\frac{a_{FeO}}{a_{CaO}} = \left(\frac{K_{Fe}}{K_{Ca}}\right) \frac{1}{h_{Ca}} \tag{4.7}$$

$$h_{Ca} = WCa\, f_{Ca} \tag{4.8}$$

Further,

$$f_{Ca} = 10^{(e_{Ca}^{Ca} \times WCa + e_{Ca}^{C} \times WC + e_{Ca}^{O} \times WO)} \tag{4.9}$$

$$f_{O} = 10^{(e_{O}^{Ca} \times WCa + e_{O}^{C} \times WC + e_{O}^{O} \times WO)} \tag{4.10}$$

For the temperature reported in the slag activity data and an initial value of WC and WCa, the values of f_{Ca} and f_O are calculated using equations (4.9) and (4.10). Initially the terms $(e_{Ca}^{O} \times WO)$ and $(e_{O}^{O} \times WO)$ are assumed to be zero. The h_{Ca} is calculated using equation (4.8). The

values of K_{Fe}, K_{Ca} and h_{Ca} in equation (4.7) gives a_{FeO}/a_{CaO}. Corresponding to the $\log(a_{FeO}/a_{CaO})$, using the regression equations, X_{CaO}, a_{FeO} and a_{CaO} can be found.

Considering equations (4.2) and (4.4)

$$h_O = \frac{a_{CaO}}{K_{Ca} h_{Ca}} \qquad (4.4)$$

It is known that

$$h_O = WO \times f_O \qquad (4.11)$$

From equations (4.4) and (4.11),

$$WO = \left(\frac{a_{CaO}}{K_{Ca}\ h_{Ca}\ f_O}\right) \qquad (4.12)$$

The WO obtained from equation (4.12) is iterated back to refine f_O and f_{Ca} till two consecutive values of WO agree with less than 1% error.

In the above calculation procedure, the e_O^{Ca} and e_{Ca}^O values used are those of Sponseller and Flinn.[9] Due to the uncertainty of the e_O^{Ca} and e_{Ca}^O values, the above model was altered to give the henrian activity of oxygen, h_O, corresponding to an assumed henrian activity of calcium, h_{Ca}. This is accomplished by using equations (4.7) and (4.5) along with the regression equations.

2.4.5 Discussion on the calculation models

(i) Computer programs for both the models in Sections 2.4.1 to 2.4.4 were made in FORTRAN IV language and run on the DEC1090 computer system at I.I.T., Kanpur.

(ii) Model 1 requires large number of data points of the slag activity to compute WO and WM (M = Si, Al, Ca). The value of h_O is fixed by a_{FeO}. Model 2 is more flexible since it can evaluate WO for any initial WM.

(iii) Model 1 involves solving transcendental equations simultaneously by Newton-Raphson's technique. Model 2 avoids this procedure and converges faster.

(iv) In Model 2, regression equations were used and these equations fitted well with experimental data with less than 1% error.

(v) In Model 2, the regression equations have been obtained through the use of system subroutine E02ACF from NAG subroutine library. This subroutine works only when the values on the abscissa are in strictly increasing monotonic sequence.

2.5 Results and Discussions

The results for deoxidation with manganese, for both simple (pure MnO as product) and complex deoxidations (FeO-MnO as product), are presented in Figure 5. It may be observed from this figure that equilibrium oxygen increases with increase in temperature for a fixed carbon content. With increase in carbon content the equilibrium oxygen increases at a given temperature. If one assumes the formation of FeO-MnO as the complex deoxidation product the corresponding equilibrium oxygen, when compared with pure MnO as the deoxidation product, is lower. This would be evident by comparing the broken curve with the continuous curve.

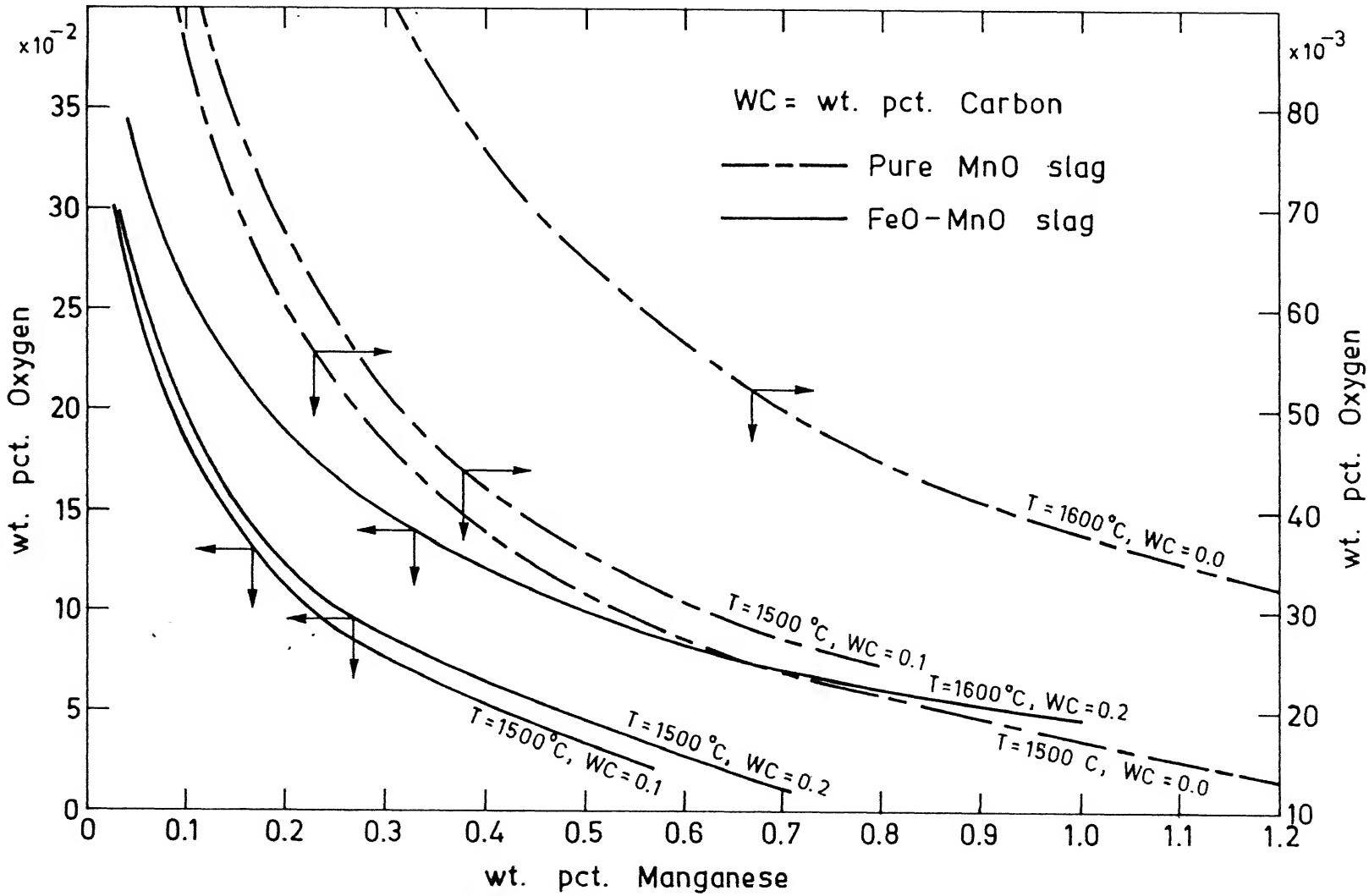

Fig. 5. Fe-Mn-O equilibria in liquid steel.

The deoxidation equilibria with silicon, assuming SiO_2 and $FeO-SiO_2$ slag is given in Figure 6. As explained in Section 2.2.2 many workers have reported that the activity of FeO in system $FeO-SiO_2$ may not vary significantly with temperature. Hence the same set of activity data have been used for temperatures between 1350°C and 1550°C. At 1600°C and above, ideal behaviour may be applied to the system suggested by Bodsworth.[5] But it was, however, not possible to obtain a simple equation of oxygen dependence on weight percent silicon as was the case for manganese, equation (1.13) in Section 2.4.1. If one compares the equilibrium silicon for a given concentration of oxygen in Figure 6, it would be clear that for the product $FeO-SiO_2$ the equilibrium values are lower by a factor of 1000 against the case when pure silica forms.

The deoxidation curves for aluminium are given in Figure 7. It may be observed that the curve for simple deoxidation (pure alumina as the deoxidation product) is smooth whereas there is scatter in the results obtained with $FeO-Al_2O_3$ as the deoxidation product. The scatter may be due to the inaccuracies in the experimental data reported by Banya et al.[22] The Figure 7 shows that the equilibrium aluminium is considerably lowered when complex $FeO-Al_2O_3$ type slag forms. However, there is a very limited range in which the calculation could be done for the case when liquid $FeO-Al_2O_3$ product forms.

In the case of deoxidation by calcium the results are shown in Figure 8 where the henrian activity of calcium

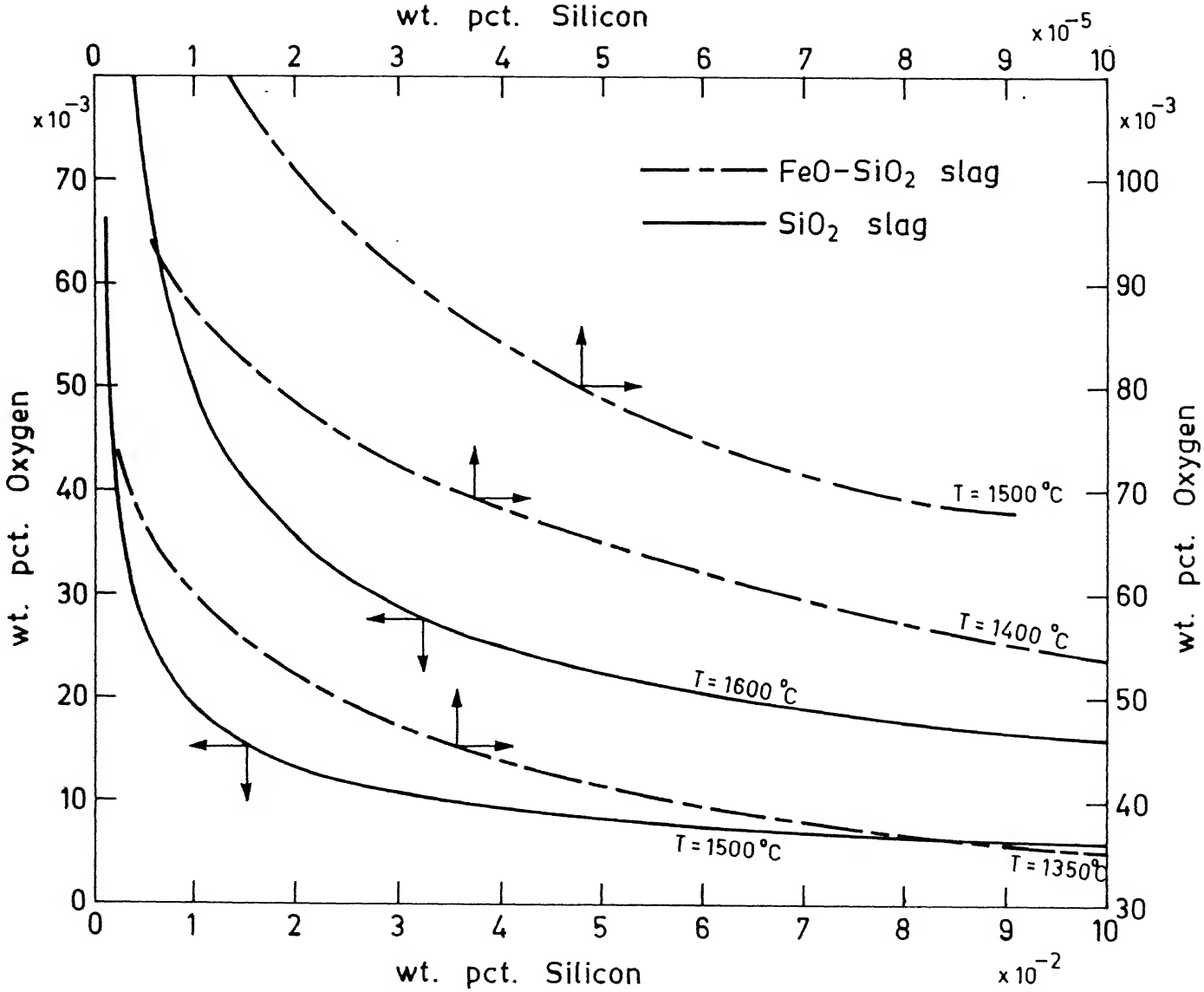

Fig. 6. Fe-Si-O equilibria in liquid steel.

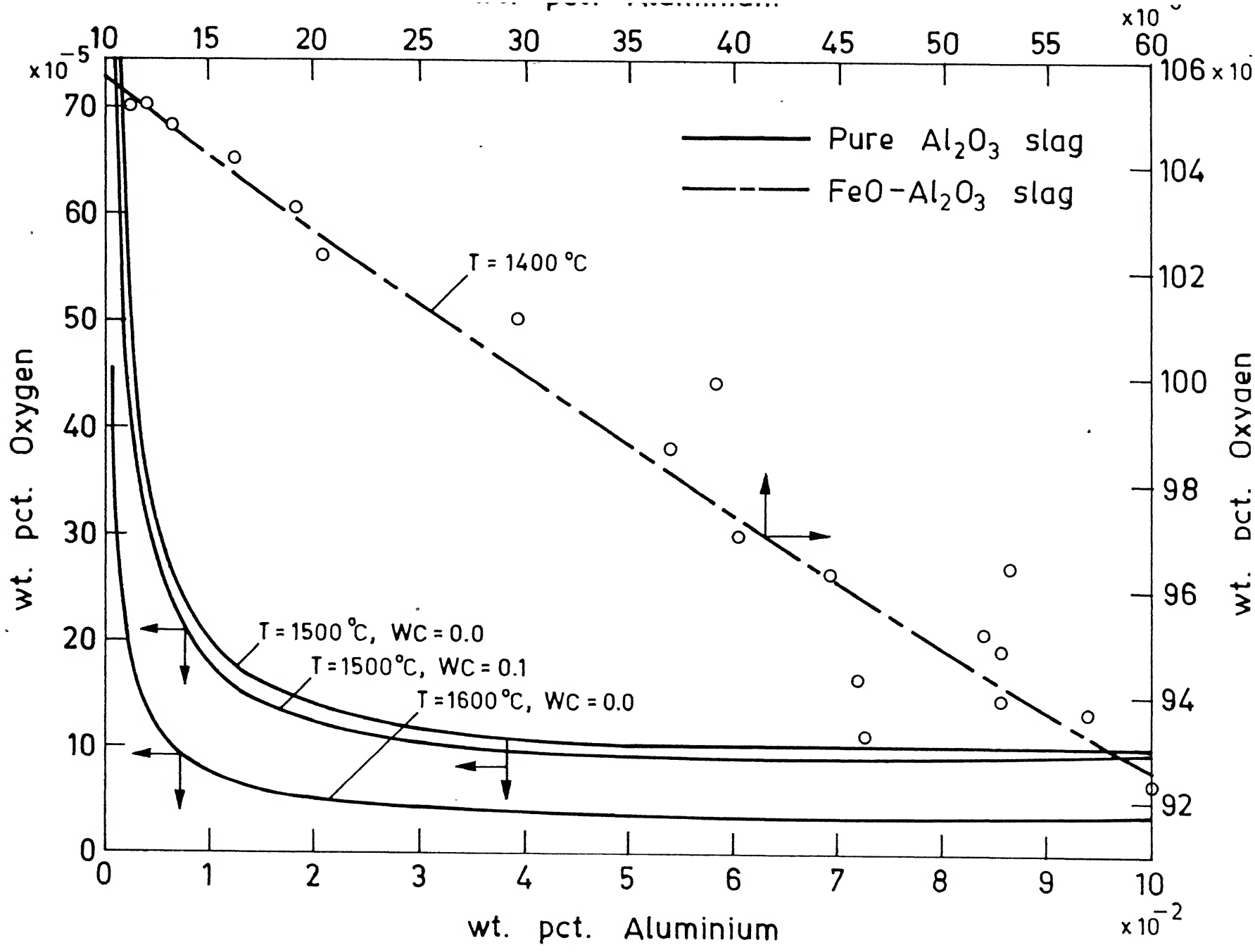
x10
10 15 20 25 30 35 40 45 50 55 60
x10⁻⁵
70 60 50 40 30 20 10 0
106 x 10
104 102 100 98 96 94 92
Pure Al2O3 slag
FeO-Al2O3 slag
T = 1400 °C
T = 1500 °C, WC = 0.0
T = 1500 °C, WC = 0.1
T = 1600 °C, WC = 0.0
wt. pct. Oxygen
wt. pct. Oxygen
0 1 2 3 4 5 6 7 8 9 10
wt. pct. Aluminium
x10⁻²

has been plotted against the henrian activity of oxygen. It was possible to calculate the weight percent oxygen corresponding to weight percent calcium only when $e_O^{Ca} = -1.4$ and $e_{Ca}^{O} = -3.6$.[9] The values reported by Kobyashi et al,[10] $e_O^{Ca} = -535$ and $e_{Ca}^{O} = -1330$, lead to negative concentrations of calcium by Model 1. When Model 2 was used the f_O value in equation (4.10) progressively decreases in each step of the iteration to refine the f_i values. This lead to higher values of oxygen in equation (4.12)

Faulring and Ramalingam[11] came across a similar difficulty. Kobyashi et al[10] has obtained one set of experimental data on calcium-oxygen equilibria. They observe that the deoxidation power of calcium has been hardly estimated due to the deoxidising action of other elements. They studied the dependence of oxygen in metal against the effective amount of calcium added. It showed linearity in the range of high oxygen content $[O] > 150$ ppm and exponential relation in the low oxygen range $[O] < 100$ ppm. The simple deoxidation equilibria calculation for this system gave a straight line with large negative slope instead of the exponential variation. Hence it was not possible to compare it with calcium deoxidation producing FeO-CaO slag. The results of the FeO-CaO system showed that the henrian activity of calcium decreased drastically when compared to that of Kobyashi et al.[10]

In the case of calcium and aluminium it was not possible to study the effect of temperature due to the lack of slag activity data at various temperatures.

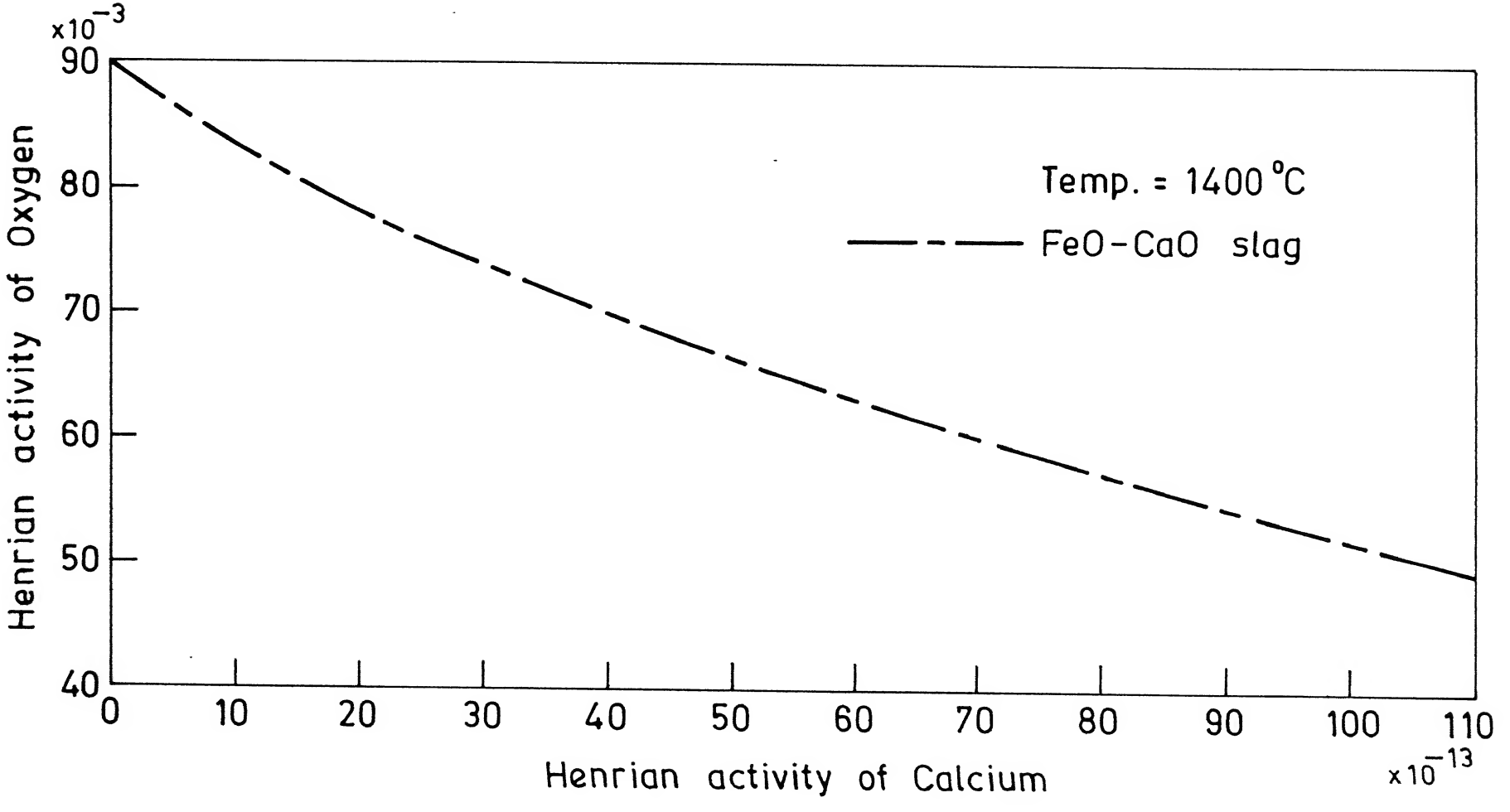

Fig. 8. Fe-Ca-O equilibria in liquid steel.

Chapter 3

THERMODYNAMIC EQUILIBRIA IN Mn-Si, Ca-Si, Ca-Al AND Ca-Mn DEOXIDATION

3.1 Introduction

In this chapter the deoxidation equilibria in systems Fe-Mn-Si-O, Fe-Ca-Si-O, Fe-Ca-Al-O, and Fe-Ca-Mn-O have been studied. In the case of Fe-Mn-Si-O and Fe-Ca-Si-O it was possible to study the effect of FeO as well. For Fe-Ca-Al-O systems the study is limited to the CaO-Al_2O_3 slags only. Further, in the case of Fe-Ca-Mn-O system the investigation has been carried out only for FeO-CaO-MnO type slags. The thermodynamic model in each case requires activity-composition data for the respective slag systems. Therefore, a detailed literature survey has been carried out for each system to obtain the data for thermodynamic calculations.

3.2 Equilibria in Silicon-Manganese Deoxidation

3.2.1 Literature review on Fe-Mn-Si-O equilibria

Bell et al[24] studied the distribution of manganese and oxygen between molten iron and FeO-MnO-SiO_2 slags. From this equilibrium data, activities of MnO and SiO_2 in MnO-SiO_2 slags were determined. They calculated the manganese concentration at 1500°C from

$$\% \text{ Mn} = \frac{\gamma_{MnO}(\Sigma \text{ MnO})}{3.8(\Sigma \text{ FeO})}$$

$$= \frac{\text{MnO}}{K'_{Mn}(\Sigma \text{ FeO})} \qquad (3.2.1)$$

where,

$$K'_{Mn} = \frac{3.8 \times \gamma_{FeO}}{\gamma_{MnO}}$$

Σ MnO = Total manganese oxide content of the deoxidation product

Σ FeO = Total iron oxide content of the deoxidation product.

The equilibrium silicon is given as,

$$\% \text{ Si} = 4.5 \frac{a_{SiO_2}}{(\Sigma \text{ FeO})^2} \qquad (3.2.2)$$

with the assumption that activity of FeO is proportional to weight percentage FeO. The results of equations (3.2.1) and (3.2.2) were lower when compared with those of Hilty and Crafts. Highest silicon contents were obtained with a silica saturated FeO-MnO-SiO_2 slag in equilibrium with manganese in steel.

Abraham et al[25] measured activities of MnO in silicate melts. The activity of MnO in MnO-SiO_2 were substantially greater than those estimated by Bell et al[24] at 1550°C. This was attributed to the simplifying assumption made by Bell and coworkers[24] that $_{FeO}$ was unity in FeO-MnO-SiO_2-MgO slags. From the activity data of FeO-SiO_2 and MnO-SiO_2, they further calculated a_{MnO}/a_{FeO} ratio using the ideal mixing laws proposed by Richardson and obtained activity values that were comparable with the experimental results of Bell et al.[24]

Scimar[26] obtained the activity-composition diagram for the ternary system FeO-MnO-SiO_2. Activities in the binaries FeO-MnO, FeO-SiO_2 and MnO-SiO_2 were plotted in the

liquidus range. . The experimental data obtained by Bell et al[24] and that of Chipman and Winkler were incorporated and the activity curves for FeO and MnO were obtained by extrapolation assuming slight positive deviation. The diagram thus obtained was used in deoxidation calculations. From the known slag composition the composition of metal and the amount of deoxidisers (Si and Mn) to be added could be found.

Walsch and Ramachandran[27] used the data of Hilty and Crafts on the oxygen solubility in liquid iron containing Si and Mn and the activity data of Chipman and Winkler on the activity of $MnO-SiO_2$ melts to obtain the expression,

$$\log a_{<SiO_2>} = -6.85 + \frac{12700}{TEMP} - 0.5 \log \frac{h_{Mn}}{h_{Si}} \qquad (3.2.3)$$

Bell[28] calculated activity of ferrous oxide in $FeO-MnO-SiO_2$ slags using silica crucible for silica saturated slags and magnesia crucible for slags without silica saturation. From the slag metal analysis they calculated a_{FeO}. Using the data from $FeO-SiO_2$ and $MnO-SiO_2$ binaries, from ideal silicate mixing model they calculated activities of MnO, SiO_2 and FeO. Their experimental data confirmed the applicability of ideal mixing laws. From this they calculated manganese and silicon in equilibrium with oxygen, which allowed the determination of composition of the deoxidation product for a given residual manganese and silicon content.

Fischer and Bardenheuer[29] did experiments at 1530°C, 1600°C and 1700°C to study the slag metal equilibria in system $FeO-MnO-SiO_2$. They obtained activity of FeO for a

given saturation in FeO-MnO solid solution. Their activities of FeO and MnO in relation to activity of SiO_2 at 1530°C are given in Reference 42.

Meysson and Rist[30] applied the ideal silicate mixing model to the FeO-MnO-SiO_2 slag system. They used the activity composition data of the binaries FeO-SiO_2 and SiO_2-MnO and the experimental data from Bell [28] They accounted for the deviations from ideality. The experimental data points showed a considerable scatter from the isoactivity curves obtained by calculation.

Herty and Fitterer[31] found that the fluidity of liquid slag is governed by an optimum Mn/Si ratio in deoxidations with manganese and silicon. A ratio between 4 and 7 gives fluid silicates. According to Korber and Oelsen[31] the Mn/Si ratio needed to obtain fluid silicate decreases with increasing silicon and manganese contents.

Fujita and Maruhashi[32] carried out experimental work on equilibrium between molten iron and FeO-MnO, FeO-MnO-SiO_2 slags at 1560°C in a rotating crucible furnace. From the slag-metal equilibria on FeO-MnO and the heat of fusion of FeO they determined the heat of fusion of MnO. They applied regular solution model to the FeO-MnO-SiO_2 slag and obtained the interaction parameter values for the FeO-MnO:0, FeO-SiO and MnO-SiO by regular solution equation. The isoactivity lines obtained for MnO and FeO agreed well with the experimental data of Bell.[28] However, the agreement was not good for silica activity. The values of activity of SiO_2 were a

little lower than found experimentally. They calculated the equilibrium Mn, Si and O in metal for a given slag composition and observed that for a given manganese in iron, the oxygen in iron decreases with silicon. For a given silicon content the oxygen in iron remained constant, if the product formed is solid silica + (FeO - MnO - SiO_2) melt. If the product formed is silica saturated FeO-MnO-SiO_2 slag then the oxygen in iron decreases with manganese for a given silicon.

Sommerville et al[33] applied regular solution theory to the FeO-MnO-SiO_2 slags as done by Fujita and Maruhashi.[32] The interaction coefficients used for FeO-SiO_2, MnO-SiO_2 and FeO-MnO differed to some extent due to the different choice of standard states. The activities of FeO and MnO obtained by them agree well with experimental data. Activity coefficients γ_{FeO} and γ_{MnO} were expressed as functions of the composition of the slag as,

$$\log \gamma_{FeO} = - 1.2 X^2_{SiO_2} + 1.0 X_{MnO} X_{SiO_2} + 0.11 \qquad (3.2.4)$$

$$\log \gamma_{MnO} = - 2.2 X^2_{SiO_2} - 1.0 X_{FeO} X_{SiO_2} \qquad (3.2.5)$$

where X_i = mole fraction of component i.

Jacquemot and Gatellier[34] have experimentally studied the manganese, silicon, oxygen equilibria in metal after deoxidation by manganese and silicon. It was observed that decantation of inclusion becomes very fast when Mn/Si ratio is 5. The mathematical approach to obtain the equilibrium contents of manganese, silicon and oxygen in iron from the slag composition of FeO-MnO-SiO_2 slag was discussed and

the results of the various workers on Fe-Mn-Si-O equilibria were compared.

Wanibe Yashimoto et al[35] determined activity of FeO in the $FeO-MnO-SiO_2$ slags in the temperature range 1250 to 1350°C. They obtained activity of FeO by measuring the activity of oxygen in a bath of silver in equilibrium with molten slag using solid electrolyte.

Fujisawa and Sakao[36] have studied the quarternary $FeO-MnO-SiO_2-Al_2O_3$ as an extension of the work of Sommerville et al.[33] Experiments were conducted with Al_2O_3 saturated $MnO-SiO_2-Al_2O_3-FeO$ slag in equilibrium with molten iron. Using these data along with the data from the ternaries the Regular solution model was applied to the above quarternary to obtain,

$$\log \gamma_{FeO} = -1.2 X_{SiO_2} - 0.05 X^2_{AlO_{1.5}} + 1.0 X_{MnO} X_{SiO_2} + 0.55 X_{MnO} X_{AlO_{1.5}} + 0.25 X_{SiO_2} X_{AlO_{1.5}} + 0.11 \quad (3.2.6)$$

$$\log \gamma_{MnO} = -2.2 X^2_{SiO_2} - 0.6 X^2_{AlO_{1.5}} - 1.0 X_{FeO} X_{SiO_2} - 0.55 X_{FeO} X_{AlO_{1.5}} - 1.3 X_{SiO_2} X_{AlO_{1.5}} \quad (3.2.7)$$

$$\log \gamma_{SiO_2} = -1.2 X_{FeO} - 2.2 X^2_{MnO} - 1.5 X^2_{AlO_{1.5}} - 3.4 X_{FeO} X_{MnO} - 2.65 X_{FeO} X_{AlO_{1.5}} - 3.1 X_{MnO} X_{AlO_{1.5}} \quad (3.2.8)$$

where,

γ_i = activity coefficients of component i

X_i = mole fraction of component i.

It should be observed that when $X_{AlO_{1.5}} = 0$, the equations (3.2.6) and (3.2.7) reduce to equations (3.2.4) and (3.2.5) obtained by Sommerville et al[33] for $FeO-MnO-SiO_2$ ternary system.

Korousic Ljubljana[37] obtained deoxidation balance of the steel melt with Mn, Si and as well with Mn, Si and Al, using equation (3.2.3) of Walsch and Ramachandran.[27] The activity of oxygen as a function of activity of silicon and manganese was expressed as

$$h_O = \frac{10^{(-9170/T + 2.585)}}{(h_{Si} h_{Mn})^{0.25}} \qquad (3.2.9)$$

For the equilibrium Mn, Si, Al and O the interdependence was given by,

$$h_O = h_{Mn} \cdot h_{Si}\, 10^{\left(\frac{36676}{TEMP} - 10.34\right)} + h_{Al} \cdot h_{Si}\, 10^{\left(\frac{62076}{TEMP} - 21.82\right)} - 0.25 \qquad (3.2.10)$$

Composition of the inclusions formed in the equilibria Fe-Mn-Si-O was calculated and compared with experimental results, showed good agreement.

Palmaers et al [38] proposed thermodynamic models on deoxidation by manganese and silicon involving $FeO-MnO-SiO_2$ type products and Mn-Si-Al involving $MnO-SiO_2-Al_2O_3$ type products. Using Scimar's[26] activity data for $FeO-MnO-SiO_2$ slag with changed reference state of liquid MnO to solid MnO obtained the following functional forms,

$$a_{FeO} = F_1(X_{FeO}, X_{MnO}, X_{SiO_2}, T) \qquad (3.2.11)$$

$$a_{MnO} = F_2(X_{FeO}, X_{MnO}, X_{SiO_2}, T) \quad (3.2.12)$$

$$a_{SiO_2} = F_3(X_{FeO}, X_{MnO}, X_{SiO_2}, T) \quad (3.2.13)$$

In the range where $X_{FeO} \simeq 0.0$ to 0.4 the following relationship was found valid

$$a_{MnO} \cdot a_{SiO_2} = K_1(T) \quad (3.2.14)$$

From equilibrium considerations the activity of oxygen as a function of activities of manganese and silicon was given as

$$h_O = \left(\frac{K_1(T) \cdot K_{Mn} \cdot K_{Si}}{h_{Mn} \cdot h_{Si}}\right)^{1/3} \quad (3.2.15)$$

where, K_{Mn} and K_{Si} are the equilibrium constants for

$$\underline{Mn} + \underline{O} = MnO(s)$$

and

$$\underline{Si} + 2\underline{O} = SiO_2(s)$$

reactions respectively.

Gaskell[39] recalculated the activity of MnO in $MnO-SiO_2$ melts from the activities of manganese at 1500°C and 1600°C as obtained by Smith and Davies. The recalculated values of activity of MnO are as much as 25% lower than the original value reported by Abraham et al.[25] Gaskell[39] obtained activity of MnO using Polymerisation model of the binary silicate melts and found good agreement with experimental data.

Rankin[40] observed that the activity data for $MnO-SiO_2$ system obtained by Abraham et al[25] and Richardson and Mehta closely agreed except that the latter study indicated a higher silica saturation level. The latter work is in agreement with Rankin's own calculation of activity of MnO.

Rankin recalculated the data of Smith and Davies keeping in view the higher saturation level of SiO_2 and found that activity of MnO differed only slightly when compared with values of Gaskell.[39] However, the activity of SiO_2 values were significantly different.

In view of the above uncertainties in activity of MnO, Rao and Gaskell[41] have performed equilibrium studies on MnO-SiO_2 slags at 1400, 1500 and 1600°C. It was observed that the activities of MnO obtained were significantly lower than the previous studies, although exact agreement existed between activity of MnO at silica saturation obtained in their study and that measured by Mehta and Richardson. Good agreement existed between the corresponding silica solubilities.

3.2.2 Scope of present work in Fe-Mn-Si-O equilibria

In the present study the data source of Abraham et al[25] (Table 8) have been used for the Mn-Si deoxidation forming MnO-SiO_2 type slag. However, it is possible to use the data of Gaskell et al[41] in the same calculation. For Mn-Si deoxidation producing complex slag of the type FeO-MnO-SiO_2, it is difficult to make decision as to which data source is correct. So the calculation was done using all the data sources. These data sources are compiled in Table 9. The various activity-composition diagrams obtained for the slag system FeO-MnO-SiO_2 are given in Figure 9 to Figure 11. From the first three data sources, the points where the three isoactivity curves of FeO, MnO and SiO_2 meet are marked and their corresponding mole fractions are found. This is compiled

Table 8

ACTIVITY-COMPOSITION DATA FOR $MnO-SiO_2$ SLAG [25]

	Temperature			
	1500°C		1650°C	
X_{MnO}	a_{MnO}	a_{SiO_2}	a_{MnO}	a_{SiO_2}
0.45	-	-	0.120	0.905
0.50	0.215	0.875	0.175	0.645
0.60	0.425	0.380	0.345	0.290
0.70	0.825	0.115	0.650	0.090
0.74	1.000	0.070	0.780	0.055
0.805	-	-	1.000	0.025

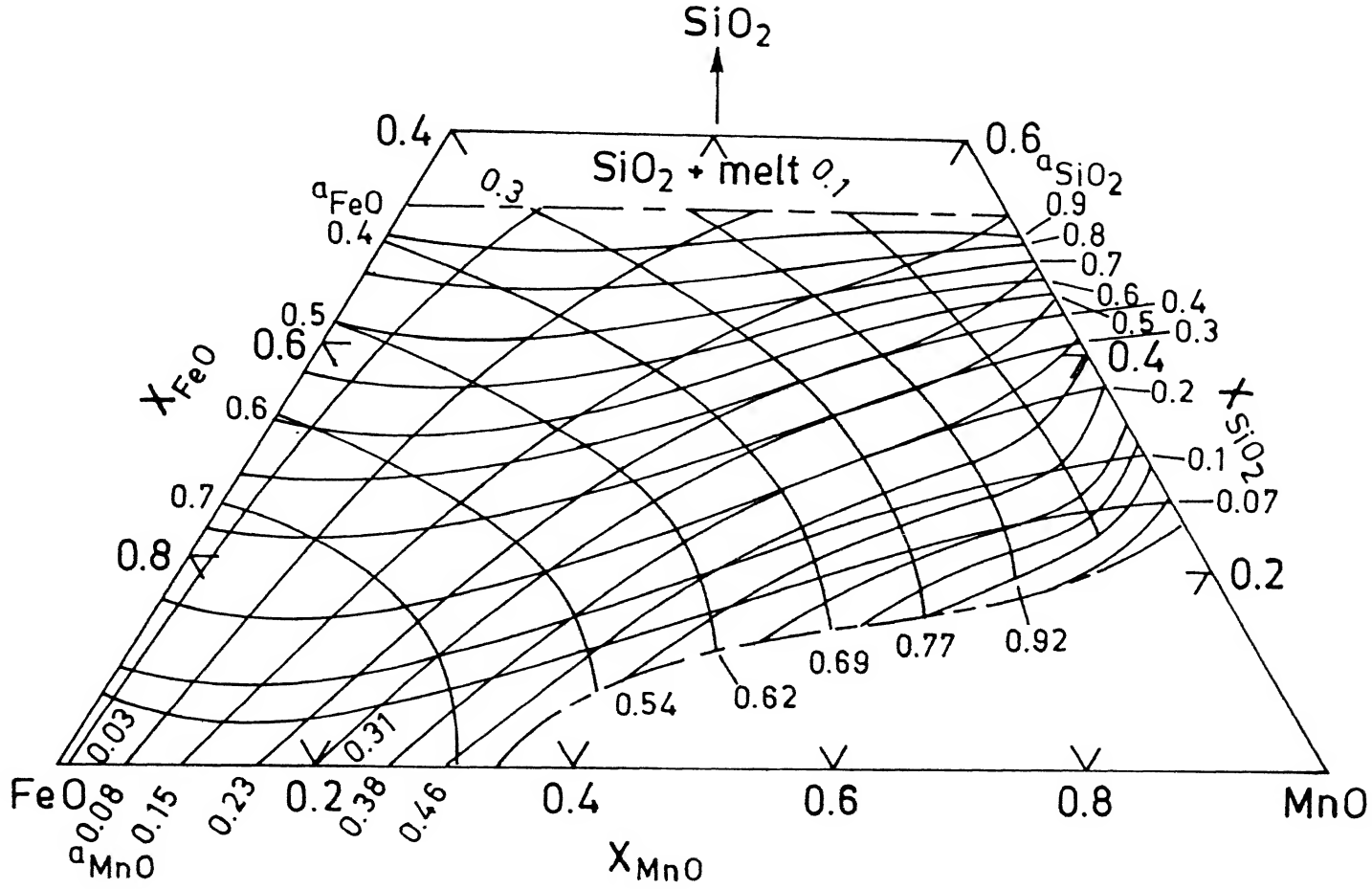

Fig. 9. Scimar's activities of oxides in $FeO-MnO-SiO_2$ melts at 1550 °C.

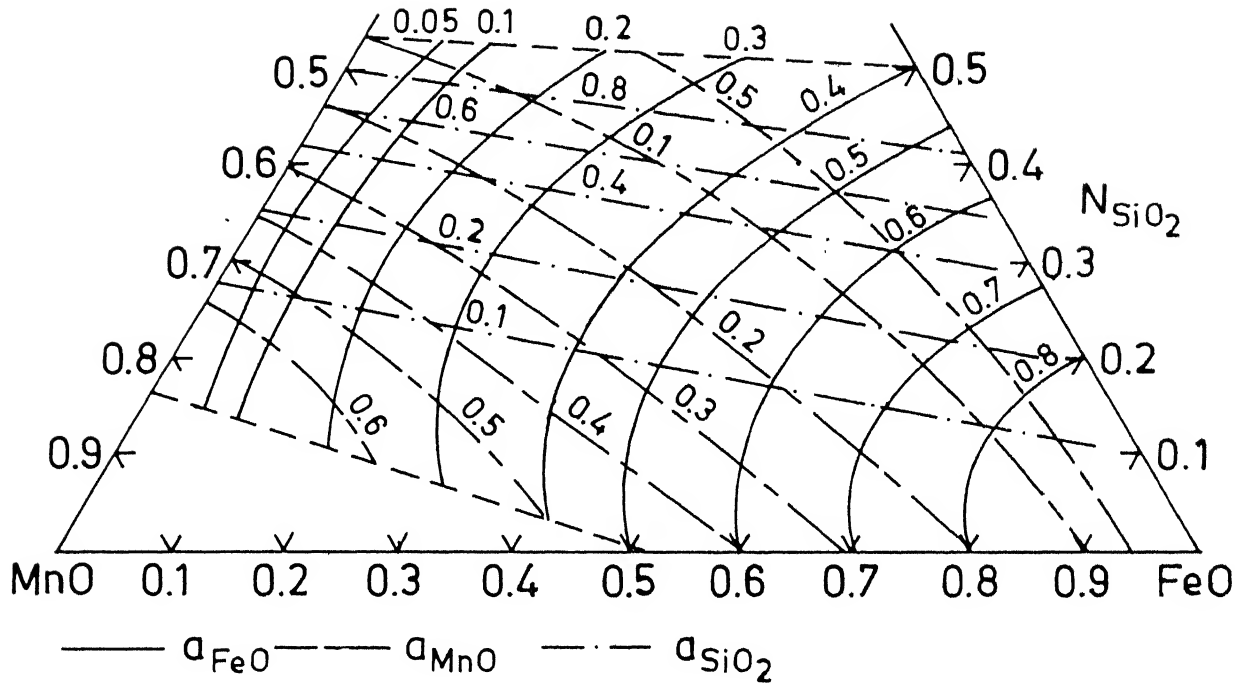

Fig. 10. Bell's isoactivity data for system $FeO-MnO-SiO_2$ at 1550 °C.

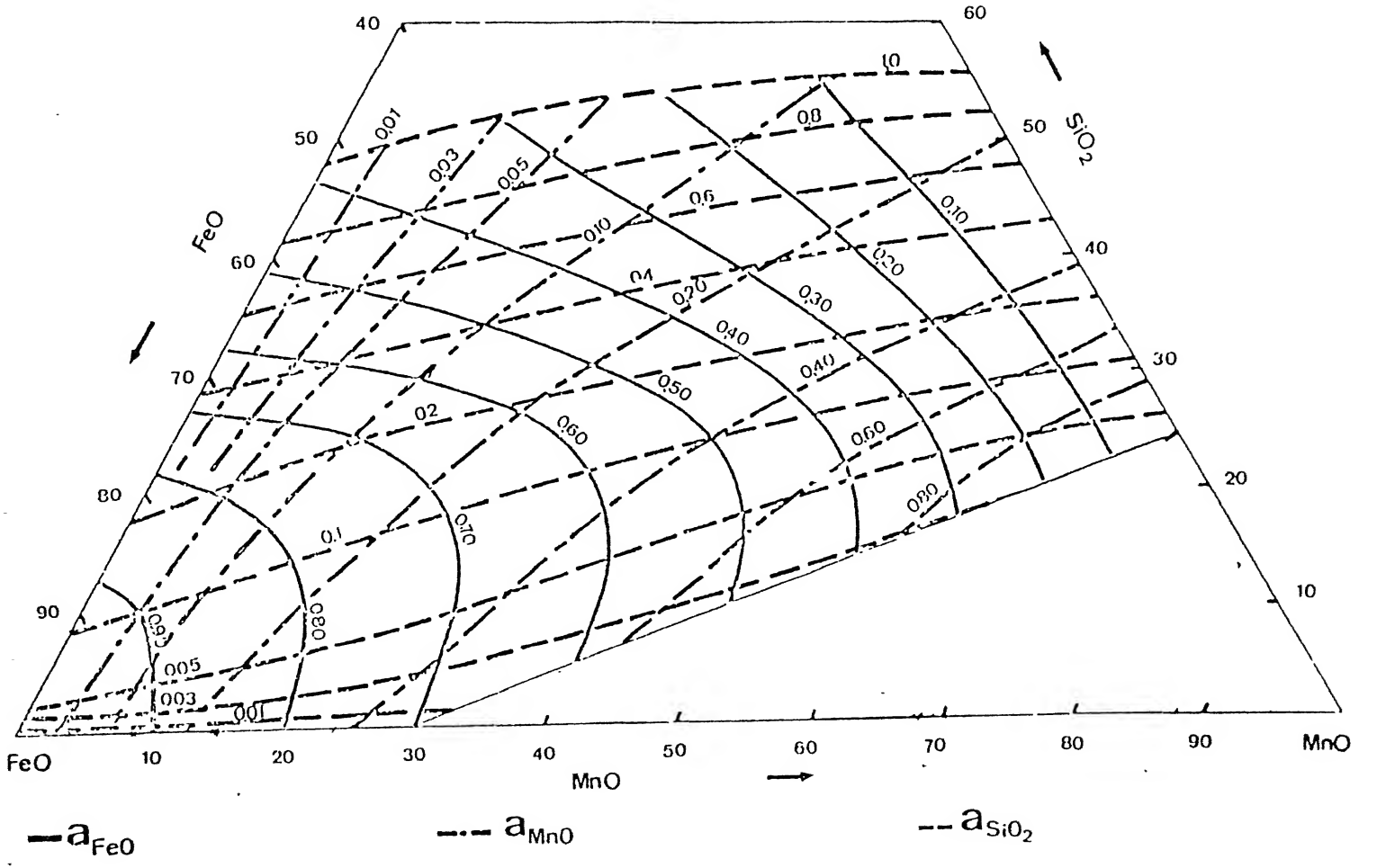

Fig. 11. Rist and Meysson's activity of oxides in $FeO-MnO-SiO_2$ system at 1550 °C

Table 9

VARIOUS SOURCES OF ACTIVITY-COMPOSITION DATA ON $FeO-MnO-SiO_2$ SLAG SYSTEM AT 1550°C

Sl.No.	Authors	Basis of the data	Figure No.	Table No.	Reference No.
1.	Scimar	Analytical equations giving best fit lines of experimental data	9	10	26,43
2.	Bell	Ideal silicate mixing theory	10	11	28
3.	Rist and Meyson	Ideal silicate mixing theory	11	12	30,34
4.	Fujisawa and Sakao	Analytical equations developed for $FeO-MnO-SiO_2-Al_2O_3$ quarternary, using regular solution theory in which molefraction of Al_2O_3 is zero	-	-	36

Table 10

ACTIVITY-COMPOSITION DATA FOR $FeO-MnO-SiO_2$ SLAG OBTAINED FROM SCIMAR[26], FIGURE 9

Sl. No.	X_{SiO_2}	X_{MnO}	X_{FeO}	a_{FeO}	a_{MnO}	a_{SiO_2}
1.	0.123	0.521	0.356	0.600	0.460	0.070
2.	0.158	0.425	0.415	0.500	0.540	0.070
3.	0.219	0.144	0.637	0.200	0.620	0.070
4.	0.247	0.062	0.691	0.100	0.690	0.070
5.	0.110	0.644	0.246	0.700	0.310	0.100
6.	0.171	0.418	0.411	0.500	0.460	0.100
7.	0.281	0.062	0.657	0.100	0.540	0.100
8.	0.178	0.527	0.295	0.600	0.310	0.200
9.	0.260	0.294	0.446	0.400	0.380	0.200
10.	0.280	0.220	0.500	0.300	0.380	0.200
11.	0.212	0.705	0.083	0.700	0.080	0.300
12.	0.329	0.233	0.438	0.300	0.310	0.300
13.	0.356	0.144	0.500	0.200	0.310	0.300
14.	0.356	0.240	0.404	0.300	0.230	0.400
15.	0.390	0.164	0.446	0.200	0.230	0.400
16.	0.322	0.658	0.020	0.600	0.030	0.500
17.	0.363	0.507	0.130	0.500	0.080	0.600
18.	0.445	0.192	0.363	0.200	0.150	0.700

Table 11

ACTIVITY-COMPOSITION DATA FOR $FeO-MnO-SiO_2$ SLAG OBTAINED FROM BELL[28], FIGURE 10

Sl. No.	X_{SiO_2}	X_{MnO}	X_{FeO}	a_{FeO}	a_{MnO}	a_{SiO_2}
1.	0.260	0.667	0.073	0.100	0.500	0.100
2.	0.233	0.547	0.220	0.300	0.400	0.100
3.	0.213	0.427	0.359	0.400	0.300	0.100
4.	0.173	0.280	0.547	0.600	0.200	0.100
5.	0.127	0.334	0.539	0.800	0.100	0.100
6.	0.026	0.120	0.854	0.430	0.200	0.200
7.	0.340	0.200	0.460	0.500	0.100	0.400
8.	0.473	0.347	0.180	0.200	0.100	0.800
9.	0.320	0.107	0.573	0.600	0.050	0.400
10.	0.373	0.127	0.500	0.500	0.050	0.600
11.	0.453	0.507	0.040	0.050	0.200	0.600

Table 12

ACTIVITY-COMPOSITION DATA FOR $FeO-MnO-SiO_2$ SLAG OBTAINED FROM MEYSSON AND RIST[30], FIGURE 11

Sl. No.	X_{SiO_2}	X_{MnO}	X_{FeO}	a_{FeO}	a_{MnO}	a_{SiO_2}
1.	0.100	0.865	0.035	0.900	0.500	0.100
2.	0.235	0.630	0.135	0.700	0.100	0.200
3.	0.310	0.605	0.085	0.600	0.050	0.400
4.	0.235	0.360	0.405	0.500	0.400	0.100
5.	0.340	0.480	0.180	0.500	0.100	0.400
6.	0.370	0.560	0.070	0.500	0.030	0.600
7.	0.435	0.480	0.085	0.400	0.030	0.800
8.	0.235	0.130	0.635	0.200	0.800	0.050
9.	0.485	0.225	0.290	0.200	0.100	0.800

Table 13

LIQUID RANGE IN M_xO_y-N_pO_q TYPE SLAG

System	Temperatures °C	Liquid range in weight percent N_pO_q		Figure No.
		From	To	
$MnO-SiO_2$	1500 1650	22.73 18.18	48.18 52.72	12
$CaO-SiO_2$	1500	44.29	65.71	13
$CaO-Al_2O_3$	1500	44.35	54.78	14

(Table 10 to Table 12) and used in the thermodynamic model to obtain the corresponding equilibrium manganese, silicon and oxygen in iron.

In the case of the fourth data source, that of Fujisawa and Sakao[36], a separate calculation was adopted to find the activities of FeO, MnO and SiO_2, using the expressions in equations (3.2.6) to (3.2.8), in which $X_{AlO_{1.5}} = 0$. These expressions are capable of finding activities of three components corresponding to a given set of slag composition within the liquid regions. This is accomplished by multiplying the activity coefficients of each component by their respective mole fraction. Thus,

$$a_{FeO} = \gamma_{FeO} \cdot X_{FeO} \qquad (3.2.16)$$

$$a_{MnO} = \gamma_{MnO} \cdot X_{MnO} \qquad (3.2.17)$$

$$a_{SiO_2} = \gamma_{SiO_2} \cdot X_{SiO_2} \qquad (3.2.18)$$

From the activity data so obtained the equilibrium manganese, silicon and oxygen in steel may be found using the general thermodynamic model developed for all the data sources.

Figure 9 was enlarged and redrafted from the original source[28]. Figure 10 was obtained by superimposing three images[43,26] and redrafted after magnification.

3.2.3 Thermodynamic model for Mn-Si deoxidation involving $MnO-SiO_2$ slag

The reactions taking place by simultaneous deoxidation by manganese and silicon are

$$\underline{Mn} + \underline{O} = MnO(s) \quad (3.1)$$

$$\underline{Si} + 2\underline{O} = SiO_2(s) \quad (3.2)$$

The equilibrium constants for the above reactions are given as,

$$K_{Mn} = \frac{a_{MnO}}{h_{Mn}\, h_O} \quad (3.3)$$

$$K_{Si} = \frac{a_{SiO_2}}{h_{Si}\, h_O^2} \quad (3.4)$$

K_{Mn} and K_{Si} as function of temperature, are given in Table 1. From equations (3.3) and (3.4),

$$\frac{a_{MnO}^2}{a_{SiO_2}} = \left(\frac{K_{Mn}^2}{K_{Si}}\right)\left(\frac{h_{Mn}^2}{h_{Si}}\right) \quad (3.5)$$

It is known that

$$h_{Mn} = f_{Mn}\, W_{Mn} \quad (3.6)$$

$$h_{Si} = f_{Si}\, W_{Si} \quad (3.7)$$

$$h_O = f_O\, W_O \quad (3.8)$$

$$f_{Mn} = 10^{(e_{Mn}^{Mn} \times W_{Mn} + e_{Mn}^{Si} \times W_{Si} + e_{Mn}^{C} \times W_C + e_{Mn}^{O} \times W_O)} \quad (3.9)$$

$$f_{Si} = 10^{(e_{Si}^{Mn} \times W_{Mn} + e_{Si}^{Si} \times W_{Si} + e_{Si}^{C} \times W_C + e_{Si}^{O} \times W_O)} \quad (3.10)$$

$$f_O = 10^{(e_O^{Mn} \times W_{Mn} + e_O^{Si} \times W_{Si} + e_O^{C} \times W_C + e_O^{O} \times W_O)} \quad (3.11)$$

From the activity-composition data for the slag system MnO-SiO_2, Table 8, third order polynomial regression equations are obtained between

$$\log\left(\frac{a^2_{MnO}}{a_{SiO_2}}\right) \quad \text{Versus} \quad \log X_{MnO}$$

$$\log\left(\frac{a^2_{MnO}}{a_{SiO_2}}\right) \quad \text{Versus} \quad \log a_{MnO}$$

$$\log\left(\frac{a^2_{MnO}}{a_{SiO_2}}\right) \quad \text{Versus} \quad \log a_{SiO_2}$$

For a fixed value of WMn, WSi, WC and the reported temperature of the slag activity data, the values of f_{Mn}, f_{Si} and f_O can be calculated using equations (3.9) to (3.11) and Table 2. Initially the terms $(e^O_i \times WO)$, where i = Mn, Si and O are assumed to be zero. Using equations (3.6) and (3.7), h_{Mn} and h_{Si} values are found subsequently. These values of h_{Mn} and h_{Si} in equation (3.5) give the value of (a^2_{MnO}/a_{SiO_2}). Taking the $\log(a^2_{MnO}/a_{SiO_2})$ and using the regression equations, the values of X_{MnO}, a_{MnO} and a_{SiO_2} are found.

From equations (3.1), (3.3), (3.8) and (3.11),

$$WO = \frac{a_{MnO}}{h_{Mn}\, f_O\, K_{Mn}} \qquad (3.12)$$

The value of WO obtained from equation (3.12) is iterated back to refine f_{Mn}, f_{Si} and f_O till two consecutive values of WO agreed within less than 0.5% error. The calculation procedure adopted here is an improvement on that done by Bagaria[6] for the same system. The procedure is simple as it avoids the Newton-Raphson's technique and converges faster. The regression equations used in the present work are higher order polynomials which gave better fit with less than 1% error. The calculation can

start with any initial value of weight percent manganese and silicon. The calculation here was limited by the liquid range of the $MnO-SiO_2$ phase diagram. The range is given in Table 1.

The same model was modified to calculate WO, for a fixed WMn value and fixed WMn/WSi ratio as,

$$WSi = WMn/Ratio \tag{3.13}$$

Computer programs for the above model is given in the Appendix 2.

3.2.4 Thermodynamic model for Mn-Si deoxidation involving $FeO-MnO-SiO_2$ slag

The basic reactions involved in forming complex slags of $FeO-MnO-SiO_2$ are,

$$Fe + \underline{O} = FeO(s) \tag{4.1}$$

$$\underline{Mn} + \underline{O} = MnO(s) \tag{4.2}$$

$$\underline{Si} + 2\underline{O} = SiO_2(s) \tag{4.3}$$

The equilibrium constants for the above reactions may be written as follows

$$K_{Fe} = \frac{a_{FeO}}{h_O \, a_{Fe}}$$

Since iron is the solvent $a_{Fe} \simeq 1$

$$K_{Fe} = \frac{a_{FeO}}{h_O} \tag{4.4}$$

$$K_{Mn} = \frac{a_{MnO}}{h_O \, h_{Mn}} \tag{4.5}$$

and

$$K_{Si} = \frac{a_{SiO_2}}{h_{Si} \, h_O^2} \tag{4.6}$$

The equilibrium constants K_{Fe}, K_{Mn} and K_{Si} as a function of temperature are compiled in Table 1. The calculation is valid within the liquid region of the ternary phase diagrams. The data from the three sources are compiled in Table 10 to Table 12.

For a fixed slag composition and known values of a_{FeO}, h_O is found using equation (4.4). This substituted in equations (4.5) and (4.6) along with a_{MnO} and a_{SiO_2} values respectively, gives h_{Mn} and h_{Si}. Now,

$$\log h_O = \log WO + e_O^O \times WO + e_O^{Si} \times WSi + e_O^{Mn} \times WMn + e_O^C \times WC \quad (4.7)$$

$$\log h_{Mn} = \log WO + e_{Mn}^O \times WO + e_{Mn}^{Si} \times WSi + e_{Mn}^{Mn} \times WMn + e_{Mn}^C \times WC \quad (4.8)$$

$$\log h_{Si} = \log WSi + e_{Si}^O \times WO + e_{Si}^{Si} \times WSi + e_{Si}^{Mn} \times WMn + e_{Si}^C \times WC \quad (4.9)$$

Using the interaction parameter values in Table 2 and for a fixed value of WC and temperature the above three equations can be solved simultaneously using Newton-Raphson's technique for the unknown values of WO, WMn and WSi. Bagaria's[6] calculation procedure was adopted for solving WO, WMn and WSi. Computer program and the results of the above calculation are compiled in the Appendix 2.

3.3 Equilibria in Calcium-Silicon Deoxidation

3.3.1 Choice of activity data

Baird and Taylor[44] have found activity of SiO_2 in the SiO_2-CaO slag system by measuring the reaction pressure in the

system

$$SiO_2 + 3C = SiC + 2CO$$

at 1450, 1500 and 1550°C. The activity-composition curve here is well established upto about $a_{SiO_2} = 0.6$ above which there is a scatter. The activity curves obtained by previous workers were somewhat flat compared to the work by Baird and Taylor,[44] who obtained a smoother and steep curve till silica saturation. In the low silica range the data of Richardson et al and Carter et al were more reliable.

Kay and Taylor[45] have obtained more accurate results in $CaO-SiO_2$ system. It was observed that above $a_{SiO_2} = 0.5$ the curve is altered. On analysing the activities at 1450, 1500 and 1550°C it becomes that for a 50°C rise in temperature the activity of silica is decreased by a factor of 0.89. Using this fact they obtained activity data at 1600°C.

Sharma and Richardson[46] experimentally determined the solubilities of calcium sulphides in melts of lime and silica at 1500 and 1550°C. The results were used to calculate activities of lime and silica in binary lime silica melts. The results agreed with previous workers.

Timucin and Morris[47] obtained the activity of FeO for $FeO-CaO-SiO_2$ system at 1450 and 1550°C by equilibrating mixtures of calcium silicate, calcium ferrite , iron silicate, lime and silica,and analysing the samples by metallographic and X-ray diffraction techniques. Here the FeO is expressed as total iron oxide ($Fe^{2+} + Fe^{3+}$). The activities of SiO_2 and CaO were found by Gibbs Duhem integration.

Kapoor and Frohberg[48] obtained the isoactivity curves for the FeO-CaO-SiO_2 system based on statistical thermodynamic treatment. The equations for this ternary and CaO-SiO_2 binary slag melts at 1600°C were derived.

Masson[49] has applied the ionic polymerisation theory on the CaO-SiO_2 and FeO-CaO-SiO_2 slags.

Wanibe Yoshimoto et al[50] determined electrochemically, the activ ity of FeO for the system FeO-CaO-SiO_2 at temperatures 1250 to 1350°C and at 1550°C.

In the present work, the data of Sharma and Richardson at 1500°C (Table 14) have been used for the equilibria giving the product slag of the type CaO-SiO_2. For the Fe-Ca-Si-O/ FeO-CaO-SiO_2 equilibria ,the data of Timucin and Morris[47] have been employed (Table 15).

The FeO-CaO-SiO_2 diagram in Figure is obtained by superimposing, two diagrams given by Turkdogan which was enlarged and redrawn. The activity-composition data were obtained in similar manner done for FeO-MnO-SiO_2 system in Section 3.2.2.

3.3.2 Thermodynamic model for Ca-Si deoxidation involving CaO-SiO_2 slag

The reactions taking place due to the simultaneous deoxidation by calcium and silicon are,

$$\underline{Ca} + \underline{O} = CaO \qquad (2.1)$$

$$\underline{Si} + 2\underline{O} = SiO_2 \qquad (2.2)$$

The equilibrium constants of the above reactions may be given as,

Table 14

ACTIVITY-COMPOSITION DATA FOR $CaO-SiO_2$ SLAG [46] AT 1500°C

Sl. No.	X_{CaO}	a_{CaO}	a_{SiO_2}
1.	0.366	0.0017	1.000
2.	1.410	0.0022	0.850
3.	0.420	0.0024	0.810
4.	0.460	0.0033	0.620
5.	0.500	0.0055	0.390
6.	0.520	0.0074	0.290
7.	0.550	0.0120	0.160
8.	0.577	0.0240	0.069

Table 15

ACTIVITY-COMPOSITION DATA FOR $FeO-CaO-SiO_2$

SLAG [47] AT 1550°C. FIGURE 15

Sl. No.	X_{CaO}	X_{SiO_2}	X_{FeO}	a_{SiO_2}	a_{CaO}	a_{FeO}
1.	0.194	0.073	0.733	0.900	0.120	0.0005
2.	0.307	0.093	0.600	0.800	0.200	0.0005
3.	0.073	0.140	0.787	0.900	0.006	0.1000
4.	0.073	0.233	0.693	0.800	0.700	0.2000
5.	0.400	0.287	0.313	0.600	0.100	0.0500
6.	0.173	0.300	0.527	0.700	0.006	0.2000
7.	0.127	0.347	0.527	0.600	0.002	0.4000

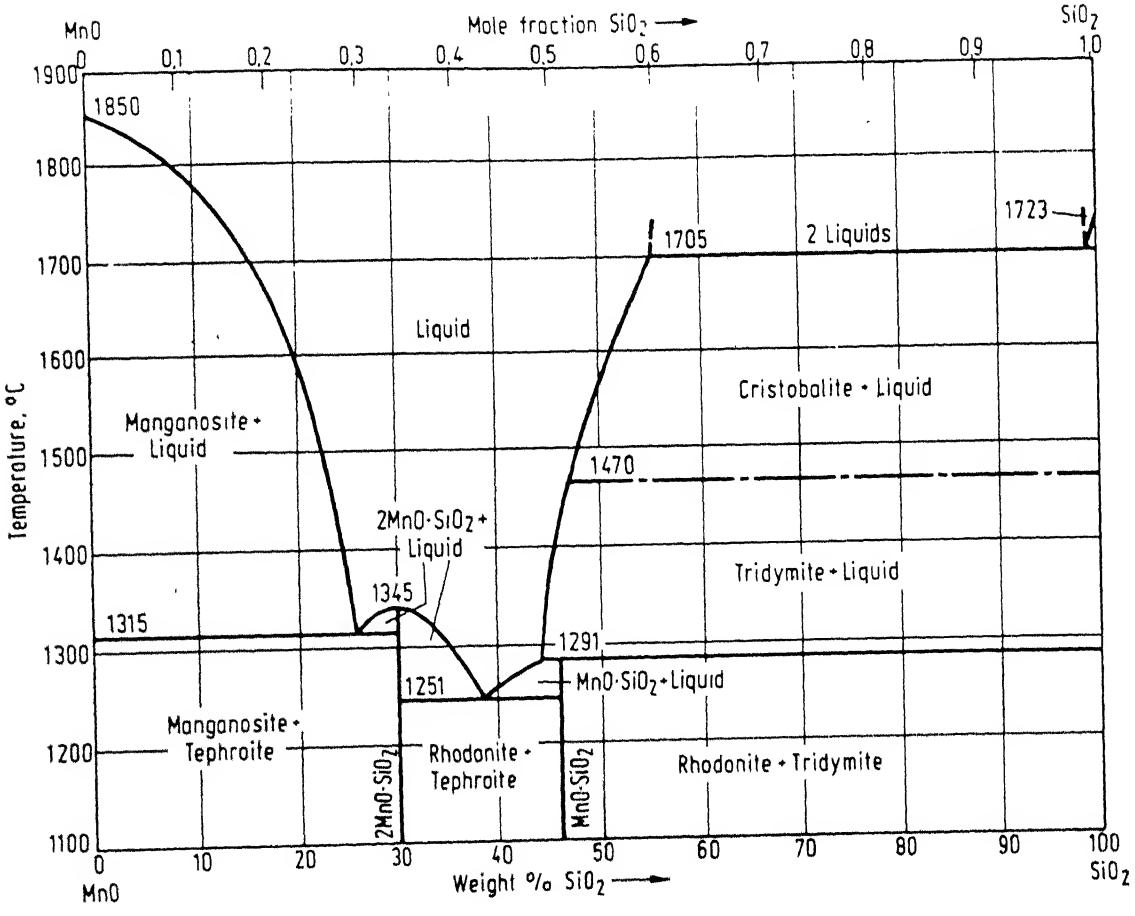

Fig. 12. Phase diagram for system $MnO-SiO_2$.

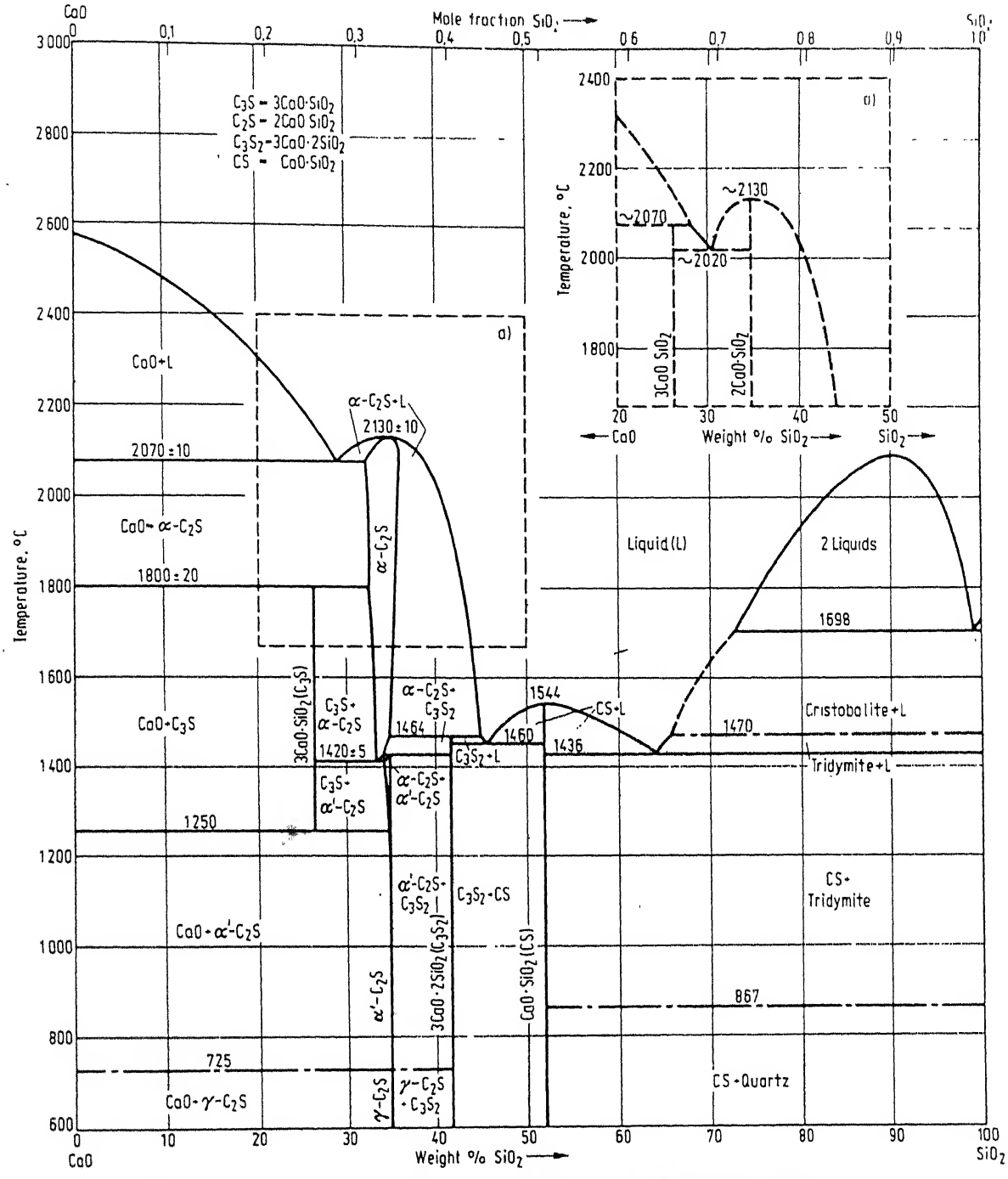

Fig. 13. Phase diagram for system CaO-SiO_2.

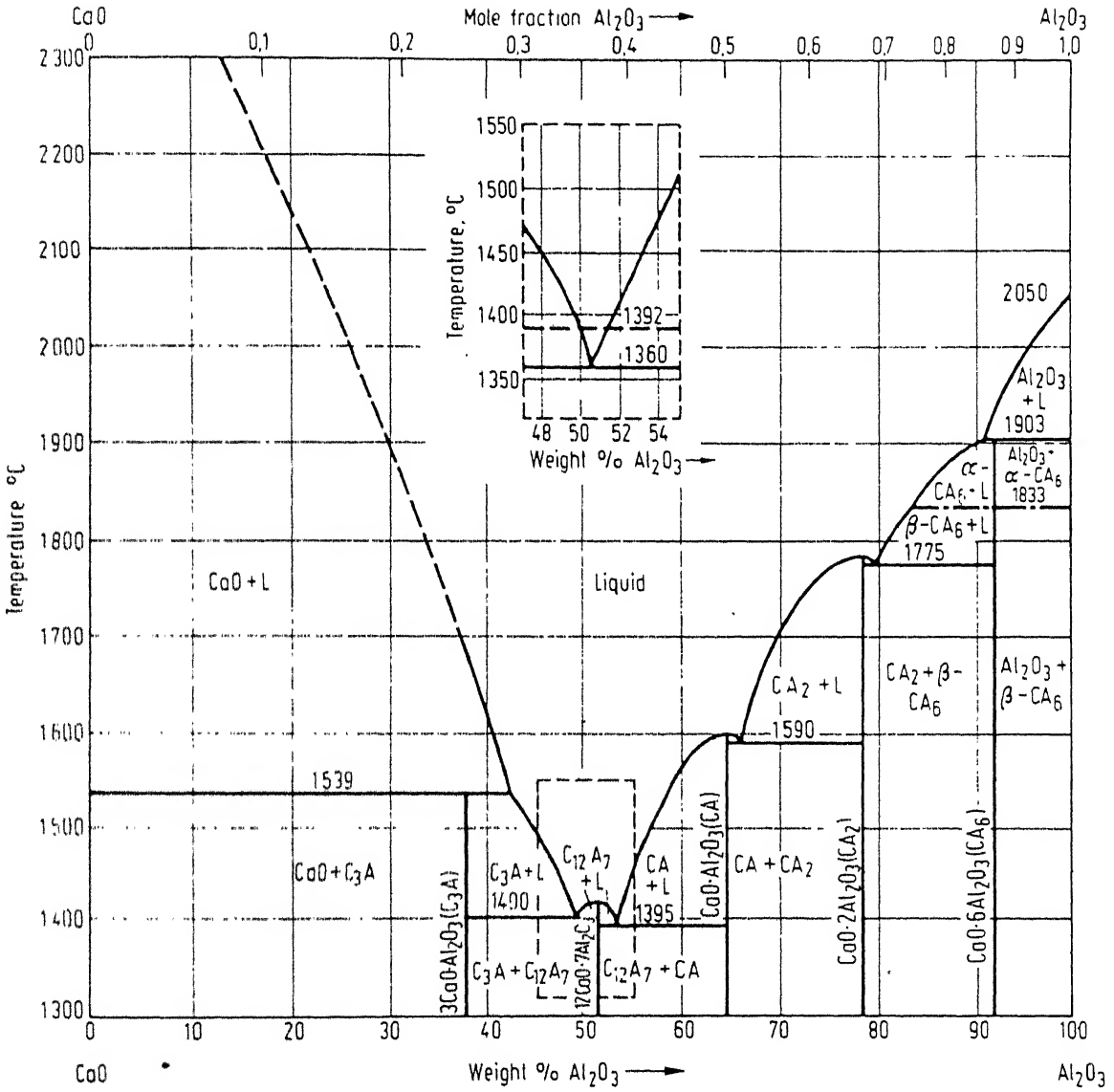

Fig. 14. Phase diagram for system CaO-Al_2O_3.

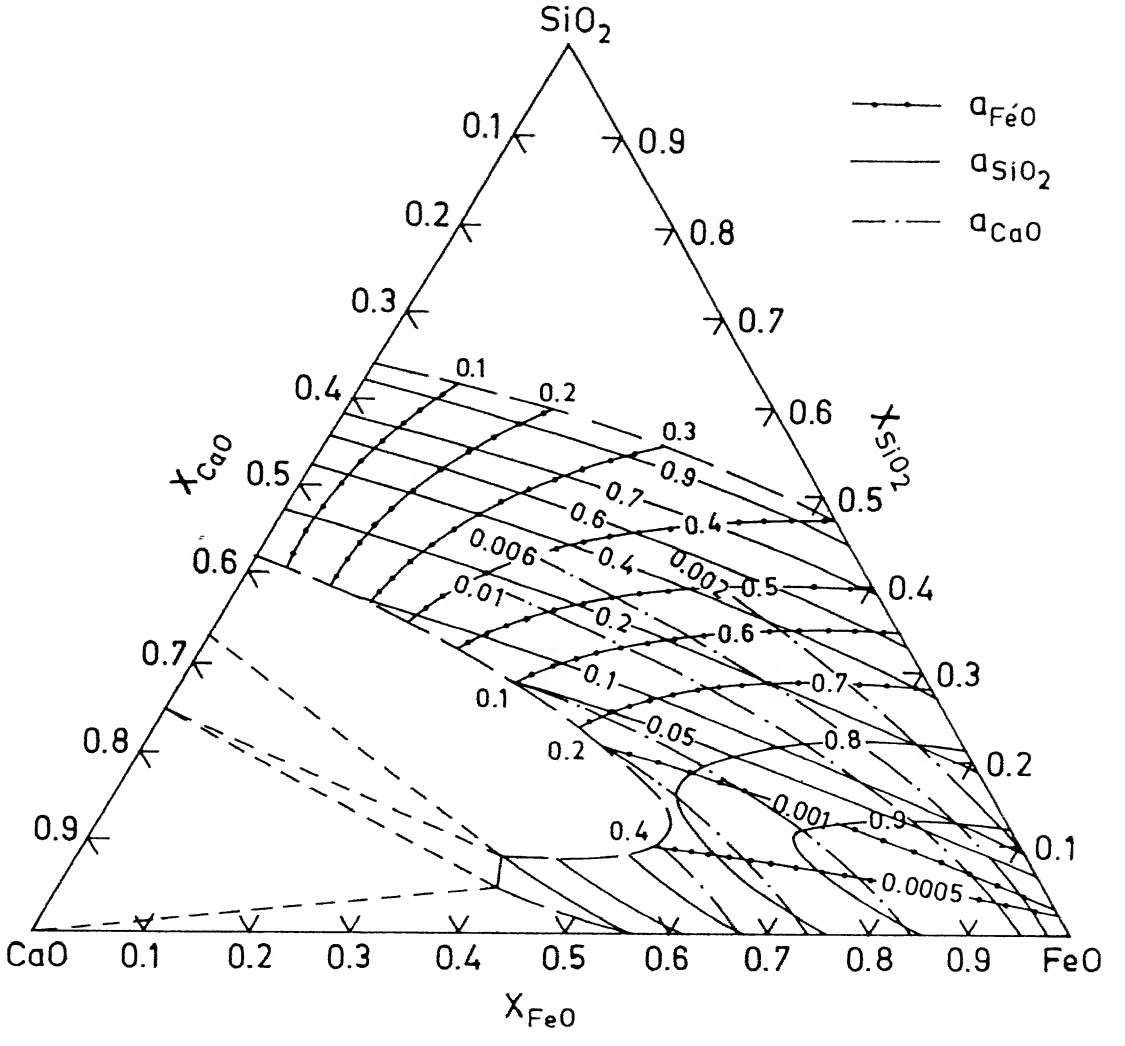

Fig. 15. Activities of oxides in FeO-CaO-SiO_2 melts at 1550 °C

$$K_{Ca} = \frac{a_{CaO}}{h_{Ca}\, h_O} \tag{2.3}$$

$$K_{Si} = \frac{a_{SiO_2}}{h_{Si}\, h_O^2} \tag{2.4}$$

The equilibrium constants K_{Ca} and K_{Si} as functions of temperature are given in Table 1.

From equations (2.3) and (2.4),

$$\frac{a_{CaO}^2}{a_{SiO_2}} = \left(\frac{K_{Ca}^2}{K_{Si}}\right) \frac{h_{Ca}^2}{h_{Si}} \tag{2.5}$$

It is known that

$$h_{Ca} = f_{Ca} \times WCa \tag{2.6}$$

$$h_{Si} = f_{Si} \times WSi \tag{2.7}$$

$$h_O = f_O \times WO \tag{2.8}$$

$$f_{Ca} = 10^{(e_{Ca}^{Ca} \times WCa + e_{Ca}^{Si} \times WSi + e_{Ca}^{C} \times WC + e_{Ca}^{O} \times WO)} \tag{2.9}$$

$$f_{Si} = 10^{(e_{Si}^{Ca} \times WCa + e_{Si}^{Si} \times WSi + e_{Si}^{C} \times WC + e_{Si}^{O} \times WO)} \tag{2.10}$$

$$f_O = 10^{(e_O^{Ca} \times WCa + e_O^{Si} \times WSi + e_O^{C} \times WC + e_O^{O} \times WO)} \tag{2.11}$$

From the activity-composition data for CaO-SiO_2 system (Table 14), fifth order polynomial regression equations are obtained between the following quantities,

$$\log\left(\frac{a_{CaO}^2}{a_{SiO_2}}\right) \quad \text{Versus} \quad \log X_{CaO}$$

$$\log\left(\frac{a_{CaO}^2}{a_{SiO_2}}\right) \quad \text{Versus} \quad \log a_{CaO}$$

$$\log\left(\frac{a^2_{CaO}}{a_{SiO_2}}\right) \quad \text{Versus} \quad \log a_{SiO_2}$$

The regression equations gave a very good fit with the experimental data with error in the range 1%.

For a fixed values of WC, WCa, WSi and the temperature of the activity-composition data, f_{Ca}, f_{Si} and f_O values are found using Table 2 and equations (2.9) to (2.11). Initially the terms (e_i^O x WO) where i = Ca, Si, O are assumed zero. The h_{Si} and h_{Ca} values are calculated using equations (2.6) and (2.7). From these values (a^2_{CaO}/a_{SiO_2}) is calculated using equation (2.5). Taking $\log(a^2_{CaO}/a_{SiO_2})$ and using the regression equations, values X_{CaO}, a_{CaO} and a_{SiO_2} are found.

Using equations (2.3), (2.8) and (2.11),

$$h_O = \frac{a_{CaO}}{h_{Ca}\, K_{Ca}} \tag{2.12}$$

or

$$WO = \frac{a_{CaO}}{h_{Ca}\, K_{Ca}\, f_O} \tag{2.13}$$

The values of WO obtained from equation (2.13) is iterated back to refine f_{Ca}, f_{Si} and f_O till two consecutive values match with less than 1% error. The calculation was performed only in the liquid range of the CaO-SiO_2 phase diagram, which is given in Table 13.

Due to the uncertainties of e_O^{Ca} and e_{Ca}^O values the henrian activities are more reliable than the weight percentages. The above model works when the e_O^{Ca} and e_{Ca}^O values of Sponseller and Flinn[9] are used. Avoiding, the use of interaction

parameter values, the same model calculates h_O value for fixed initial values of h_{Ca} and h_{Al} using equation (2.5), regression equations and (2.12). Computer program for the above model is given in Appendix 2.

3.3.3 Thermodynamic model for Ca-Si deoxidation involving $FeO-CaO-SiO_2$ slag

The reactions involved in giving $FeO-CaO-SiO_2$ complex slag are

$$Fe + \underline{O} = FeO(s) \quad (3.1)$$

$$\underline{Ca} + \underline{O} = CaO(s) \quad (3.2)$$

$$\underline{Si} + 2\underline{O} = SiO_2(s) \quad (3.3)$$

The equilibrium constants of the above reactions may be given as

$$K_{Fe} = \frac{a_{FeO}}{h_O \; a_{Fe}}$$

Since iron is the solvent $a_{Fe} \simeq 1$

$$K_{Fe} = \frac{a_{FeO}}{h_O} \quad (3.4)$$

$$K_{Ca} = \frac{a_{CaO}}{h_O \; h_{Ca}} \quad (3.5)$$

$$K_{Si} = \frac{a_{SiO_2}}{h_{Si} \; h_O^2} \quad (3.6)$$

The equilibrium constants K_{Fe}, K_{Ca} and K_{Si} as functions of temperature are compiled in Table 1. The calculation is valid only in the liquid region of the ternary phase diagram. The data for the $FeO-CaO-SiO_2$ system is compiled in Table 15.

For a fixed slag composition and known values of a_{FeO}, using equation (3.4), h_O is found. This if substituted in equations (3.5) and (3.6) along with a_{CaO} and a_{SiO_2} values respectively, gives h_{Ca} and h_{Si}. Now,

$$\log h_O = \log WO + e_O^O \times WO + e_O^{Si} \times WSi + e_O^{Ca} \times WCa + e_O^C \times WC \quad (3.7)$$

$$\log h_{Ca} = \log WCa + e_{Ca}^O \times WO + e_{Ca}^{Si} \times WSi + e_{Ca}^{Ca} \times WCa + e_{Ca}^C \times WC \quad (3.8)$$

$$\log h_{Si} = \log WSi + e_{Si}^O \times WO + e_{Si}^{Si} \times WSi + e_{Si}^{Ca} \times WCa + e_{Si}^C \times WC \quad (3.9)$$

Using the interaction parameter values in Table 2, for fixed values of WC and temperature, the above three equations can be solved simultaneously for WCa, WSi and WO using Newton-Raphson's technique done previously by Bagaria.[6] The above model works with the values of e_O^{Ca} and e_{Ca}^O recommended by Sponseller and Flinn[9] only. Due to the uncertainties in the e_O^{Ca} and e_{Ca}^O values, the same model was altered to give h_O value for an initially assumed h_{Si} and h_{Ca} values. The use of high values of e_O^{Ca} and e_{Ca}^O gave erroneous results. Computer program and the results of the above model is compiled in Appendix 2.

3.4 Equilibria in Calcium-Aluminium Deoxidation

3.4.1 Choice of activity data

Carter and Macfarlane[51] investigated the sulphur equilibrium between $CaO-Al_2O_3$ slags and $CO-CO_2-SO_2$ gas mixtures at 1500°C and the results were applied to calculate the

activities of CaO and Al_2O_3 in the system. γ_{CaS} was assumed to be constant.

Sharma and Richardson[52] determined the activity-composition data for CaO-Al_2O_3 system at 1500°C by a gas + slag equilibrium technique. They measured sulphide capacities and limiting solubilities of calcium sulphide in melts containing lime and alumina. The results obtained are lower than that of Carter and Macfarlane[51] and Chipman, due to the assumptions made earlier.

Faulring and Ramalingam[53] studied the inclusion precipitation diagram for the Fe-O-Ca-Al system. They obtained the relation between h_{Ca} and h_O in CaO-Al_2O_3 melts based on compound formation. Because of the uncertainties of e_O^{Ca} and e_{Ca}^{O} values, they have expressed all results in henrian activities.

In the present work the widely accepted[43] data of Sharma and Richardson, Table 16, has been used. The data for FeO-CaO-Al_2O_3 system is not available in the literature and hence the role of FeO in CaO-Al_2O_3 system could not be studied.

3.4.2 Thermodynamic model for the deoxidation by Ca-Al involving CaO-Al_2O_3 slags

The basic reactions taking place by the simultaneous deoxidation by calcium and aluminium are,

$$\underline{Ca} + \underline{O} = CaO(s) \qquad (2.1)$$

$$2\underline{Al} + 3\underline{O} = Al_2O_3(s) \qquad (2.2)$$

The equilibrium constants of the above reactions may be given as,

$$K_{Ca} = \frac{a_{CaO}}{h_{Ca}\, h_O} \tag{2.3}$$

$$K_{Al} = \frac{a_{Al_2O_3}}{h_{Al}^2\, h_O^3} \tag{2.4}$$

The equilibrium constants K_{Ca} and K_{Al} as functions of temperature are obtained from Table 1.

From equations (2.3) and (2.4)

$$\frac{a_{CaO}^3}{a_{Al_2O_3}} = \left(\frac{K_{Ca}^3}{K_{Al}}\right)\left(\frac{h_{Ca}^3}{h_{Al}}\right) \tag{2.5}$$

It is known that

$$h_{Ca} = f_{Ca}\, WCa \tag{2.6}$$

$$h_{Al} = f_{Al}\, WAl \tag{2.7}$$

$$h_O = f_O\, WO \tag{2.8}$$

$$f_{Ca} = 10^{(e_{Ca}^{Ca} \times WCa + e_{Ca}^{Al} \times WAl + e_{Ca}^{C} \times WC + e_{Ca}^{O} \times WO)} \tag{2.9}$$

$$f_{Al} = 10^{(e_{Al}^{Ca} \times WCa + e_{Al}^{Al} \times WAl + e_{Al}^{C} \times WC + e_{Al}^{O} \times WO)} \tag{2.10}$$

$$f_O = 10^{(e_O^{Ca} \times WCa + e_O^{Al} \times WAl + e_O^{C} \times WC + e_O^{O} \times WO)} \tag{2.11}$$

From the activity-mole fraction data in Table 16, fifth order polynomial regression equations were obtained between

$$\log\left(\frac{a_{CaO}^3}{a_{Al_2O_3}}\right) \quad \text{Versus} \quad \log X_{Al_2O_3}$$

$$\log\left(\frac{a_{CaO}^3}{a_{Al_2O_3}}\right) \quad \text{Versus} \quad \log a_{Al_2O_3}$$

$$\log\left(\frac{a_{CaO}^3}{a_{Al_2O_3}}\right) \quad \text{Versus} \quad \log a_{CaO}$$

The regression equations agreed well with the actual data with error in the range of 0.5%.

For fixed values of temperature, WC, and for assumed initial values of WCa and WAl, the values f_{Ca}, f_{Al} and f_O are calculated using equations (2.9) to (2.11) and Table 2. From equations (2.6) and (2.7), h_{Al} and h_{Ca} values are obtained. Using these values in (2.5), $(a_{CaO}^3/a_{Al_2O_3})$ can be determined. Using the $\log(a_{CaO}^3/a_{Al_2O_3})$ in the regression equations, $X_{Al_2O_3}$, $a_{Al_2O_3}$ and a_{CaO} values can be found.

From equations (2.3), (2.8) and (2.11),

$$h_o = \frac{a_{CaO}}{K_{Ca} h_{Ca}} \tag{2.12}$$

and

$$WO = \frac{a_{CaO}}{K_{Ca} h_{Ca} f_O} \tag{2.13}$$

The value of WO obtained from equation (2.13) is iterated back to refine f_{Ca}, f_{Al} and f_O values till the successive values of WO agreed within less than 1% error. The calculations in the above model was limited in the liquid range of the CaO-Al_2O_3 phase diagram, Figure 14. The liquid range is given in Table 13.

The above model works well with the e_O^{Ca} and e_{Ca}^O values recommended by Sponseller and Flinn.[9] Due to the uncertainties

of the e_O^{Ca} and e_{Ca}^{O} values the above model was modified to calculate h_O for a given initial h_{Ca} and h_{Al} values. This is accomplished using equation (2.5), regression equations and equation (2.12). The computer program for the above model is given in Appendix 2.

3.5 Equilibria in Calcium-Manganese Deoxidation

3.5.1 Choice of activity data

Tiberg and Muan[54] have determined the activities of FeO in ternary solid solutions at 1100°C by equilibrating FeO-CaO-MnO solid solutions of known composition with metallic iron. From the activity of FeO obtained from experiment, activities of CaO and MnO are found by Gibb's Duhem integration. They extrapolated their data to obtain the activity-composition data for CaO-MnO binary which showed a positive deviation from ideality. This is the only data available on CaO-MnO system. The authors are themselves not certain about the activity data of the CaO-MnO binary.

In the present work, the data for the system FeO-CaO-MnO has been used to study the Fe-Ca-Mn-O equilibria. Due to the uncertainty in CaO-MnO activity-composition data the equilibria with CaO-MnO slags has not been studied. The ternary activity composition diagram given in Figure 16 is obtained by superimposing two images which was enlarged and redrafted. The activity-composition data for this system was found in a similar manner as was done in Section 3.2.2 for FeO-MnO-SiO_2 slags. The data are compiled in Table 17.

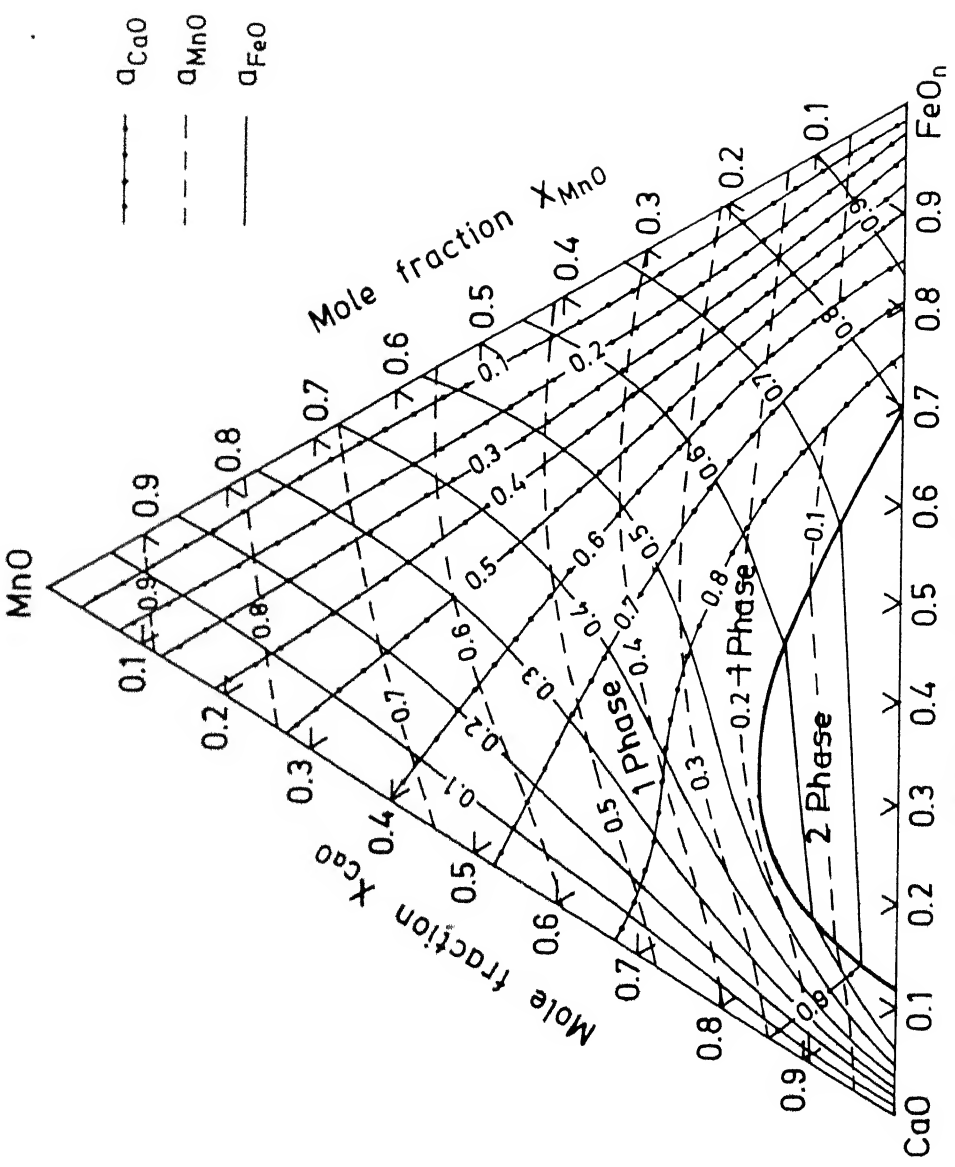

Fig. 16. Activities of oxides in FeO – CaO – MnO melts at 1100 °C.

Table 16

ACTIVITY-COMPOSITION DATA FOR $CaO-Al_2O_3$ SLAG [52] AT 1500°C

Sl. No.	X_{CaO}	a_{CaO}	$a_{Al_2O_3}$
1.	0.58	0.21	0.150
2.	0.60	0.25	0.115
3.	0.62	0.30	0.085
4.	0.64	0.38	0.060
5.	0.66	0.50	0.040
6.	0.68	0.67	0.025
7.	0.71	1.00	0.007

Table 17

ACTIVITY-COMPOSITION DATA FOR FeO-CaO-MnO SLAG [54] AT 1100°C

Sl. No.	X_{CaO}	X_{MnO}	X_{FeO}	a_{FeO}	a_{MnO}	a_{CaO}
1.	0.030	0.892	0.078	0.100	0.900	0.100
2.	0.083	0.775	0.142	0.200	0.800	0.200
3.	0.192	0.750	0.058	0.100	0.800	0.400
4.	0.125	0.642	0.233	0.300	0.700	0.300
5.	0.267	0.617	0.116	0.200	0.700	0.500
6.	0.383	0.575	0.042	0.100	0.700	0.600
7.	0.108	0.542	0.350	0.400	0.600	0.300
8.	0.225	0.525	0.250	0.300	0.600	0.500
9.	0.133	0.433	0.434	0.500	0.500	0.300
10.	0.033	0.417	0.550	0.200	0.500	0.100
11.	0.633	0.308	0.059	0.200	0.500	0.800
12.	0.042	0.325	0.633	0.700	0.400	0.100

Continued....

Table 17 (Continued):

Sl. No.	X_{CaO}	X_{MnO}	X_{FeO}	a_{FeO}	a_{MnO}	a_{CaO}
13.	0.108	0.342	0.550	0.600	0.400	0.300
14.	0.250	0.342	0.408	0.500	0.400	0.600
15.	0.517	0.283	0.200	0.400	0.400	0.800
16.	0.108	0.258	0.634	0.700	0.300	0.300
17.	0.208	0.275	0.517	0.600	0.300	0.600
18.	0.083	0.183	0.734	0.800	0.200	0.300
19.	0.183	0.200	0.617	0.700	0.200	0.600
20.	0.342	0.210	0.448	0.600	0.200	0.800
21.	0.050	0.083	0.867	0.900	0.100	0.200
22.	0.167	0.075	0.758	0.800	0.100	0.600
23.	0.842	0.058	0.100	0.600	0.100	0.900

3.5.2 Thermodynamic model for deoxidation by Ca-Mn involving FeO-CaO-MnO slags

The reactions involved in the deoxidation by calcium and manganese to produce FeO-CaO-MnO slags are,

$$Fe + \underline{C} = FeO(s) \quad (2.1)$$

$$\underline{Ca} + \underline{O} = CaO(s) \quad (2.2)$$

$$\underline{Mn} + \underline{O} = MnO(s) \quad (2.3)$$

The equilibrium constants for the above reactions may be given as

$$K_{Fe} = \frac{a_{FeO}}{h_O \, a_{Fe}}$$

since iron is the solvent $a_{Fe} \simeq 1$,

$$K_{Fe} = \frac{a_{FeO}}{h_O} \quad (2.4)$$

$$K_{Ca} = \frac{a_{CaO}}{h_{Ca} \, h_O} \quad (2.5)$$

and

$$K_{Mn} = \frac{a_{MnO}}{h_{Mn} \, h_O} \quad (2.6)$$

The equilibrium constant values as a function of temperature are given in Table 1. For known slag composition, using the a_{FeO} value in equations (2.4), the h_O value is found. The h_O value with the values of a_{CaO} and a_{MnO} in equations (2.5) and (2.6) respectively gives h_{Ca} and h_{Mn} values. Now,

$$\log h_O = \log WO + e_O^O \times WO + e_O^{Mn} \times WMn + e_O^{Ca} \times WCa + e_O^C \times WC \quad (2.7)$$

$$\log h_{Ca} = \log WCa + e^{O}_{Ca} \times WO + e^{Mn}_{Ca} \times WMn + e^{Ca}_{Ca} \times WCa + e^{C}_{Ca} \times WC \quad (2.8)$$

$$\log h_{Mn} = \log WMn + e^{O}_{Mn} \times WO + e^{Mn}_{Mn} \times WMn + e^{Ca}_{Mn} \times WCa + e^{C}_{Mn} \times WC \quad (2.9)$$

For the fixed temperature of the activity data and for fixed value of WC, the equations (2.7) to (2.9) are solved simultaneously for WCa, WMn and WO using the same procedure as was done by Bagaria[6] and in Section 3.2.4. The interaction parameters used were those compiled in Table 2. The e^{Ca}_{O} and e^{O}_{Ca} values used were those of Sponseller and Flinn.[9] The computer program for the above model is compiled in Appendix 2.

3.6 Results and Discussions

The equilibrium oxygen in metal has been calculated assuming either the formation of M_xO_y-N_pO_q type product or FeO-M_xO_y-N_pO_q type product. The details of the results obtained are presented below.

(a) Complex deoxidation by Mn, Si and Ca involving M_xO_y-N_pO_q type slags

The results of Si-Mn, Ca-Si and Ca-Al deoxidations giving the products SiO_2-MnO, CaO-SiO_2 and CaO-Al_2O_3 are shown graphically in Figure 17 to Figure 20. In the case of Si-Mn deoxidation, Figure 17, for a fixed manganese in steel hyperbolic dependence of oxygen on equilibrium silicon is observed. The results are given for two different temperatures at which the activity data are available. The results showed that

the equilibrium oxygen increased with the rise in temperature (Figure 18).

For the Ca-Si and Ca-Al deoxidations the results of equilibrium weight percentages of Ca, Si, Al and O has not been given due to the uncertainties in the e_O^{Ca} and e_{Ca}^{O} values. The results are expressed in terms of henrian activities of Ca, Si, Al and O. In the case of Ca-Si deoxidation (Figure 20), for a given henrian activity of calcium hyperbolic dependence of henrian activity of equilibrium oxygen on henrian activity of silicon is observed. In the case of Ca-Al deoxidation, for a given henrian activity of calcium, the henrian activity of oxygen decreases exponentially with henrian activity of aluminium, Figure 21. In the case of Si-Mn deoxidation, the henrian activities of the components involved are not very much different from the corresponding weight percentages. Hence, it is possible to compare the deoxidation power of the three systems Si-Mn, Ca-Si and Ca-Al with henrian activities as the criteria. The deoxidation power is greatest with Ca-Al followed by Ca-Si and Si-Mn. Both calcium and aluminium are strong deoxidisers, and they give lower equilibrium amount of oxygen in melt than in calcium and silicon as deoxidants. Since calcium is a stronger deoxidiser than manganese the equilibrium oxygen with Ca-Si as deoxidisers is lower than that with Mn-Si. The advantage of Ca-Al and Ca-Si deoxidations over simple calcium deoxidation is that when calcium alone is used it vapourises, while it is not so when Ca-Al and Ca-Si are used.

In common practice Si-Mn as deoxidisers is preferred because it results in a fluid slag product over a greater range of composition and temperature and the inclusions formed are not very detrimental to steel properties. It has been suggested in literature that [Mn]/[Si] ratio should be between 4 and 7 to get fluid slag. The effect of this ratio on equilibrium oxygen, silicon and manganese is given in Figure 19. It is observed that as [Mn]/[Si] ratio increases for the same equilibrium content of Si in steel, the equilibrium oxygen decreases. Similar effect is observed for the same in manganese content, with increasing [Mn]/[Si] ratio. Figure 19 gives equilibrium oxygen values for selected points on the [Mn]/[Si] ratio axis. When this figure is compared with the results of Korousic[37] it is found that the values of equilibrium oxygen obtained for similar Mn, Si and [Mn]/[Si] ratio are significantly higher in the present case. It may be attributed to the different calculation procedure adopted by Korousic, involving the expression (3.2.3), suggested by Walsch and Ramachandran.[27] The results obtained in the present study may be compared with the results of Turkdogan.[16] It is found that the present model gives lower contents of oxygen than predicted by Turkdogan. For 0.8 weight percent manganese and 0.2 weight percent silicon, the equilibrium oxygen is about 625 ppm lesser than that predicted by Turkdogan. This may be due to the different equilibrium constants used.

Deoxidation using Ca-Mn, involving CaO-MnO as deoxidation product has not been attempted since there is no

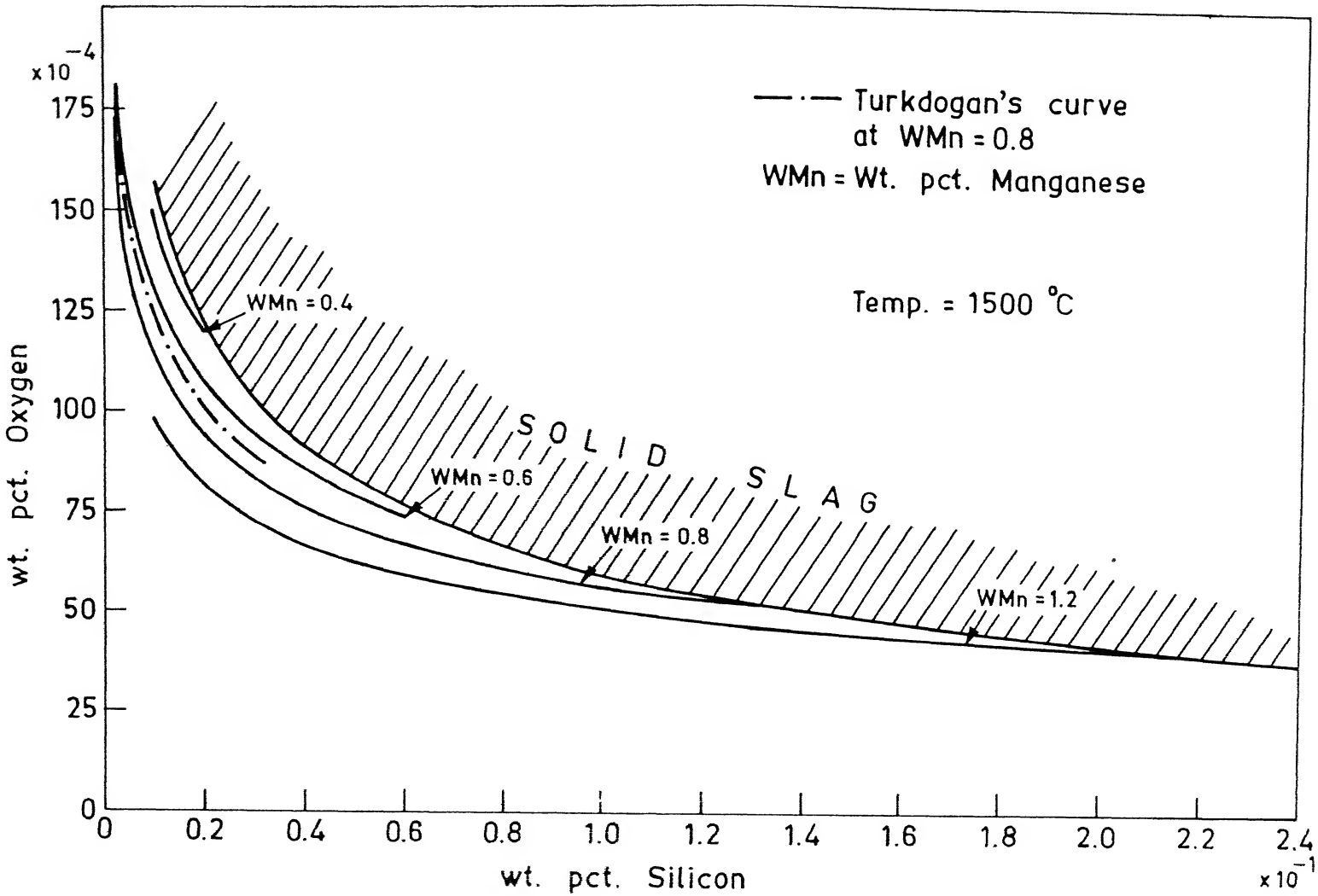

Fig. 17. Fe-Mn-Si-O equilibria in complex deoxidation.

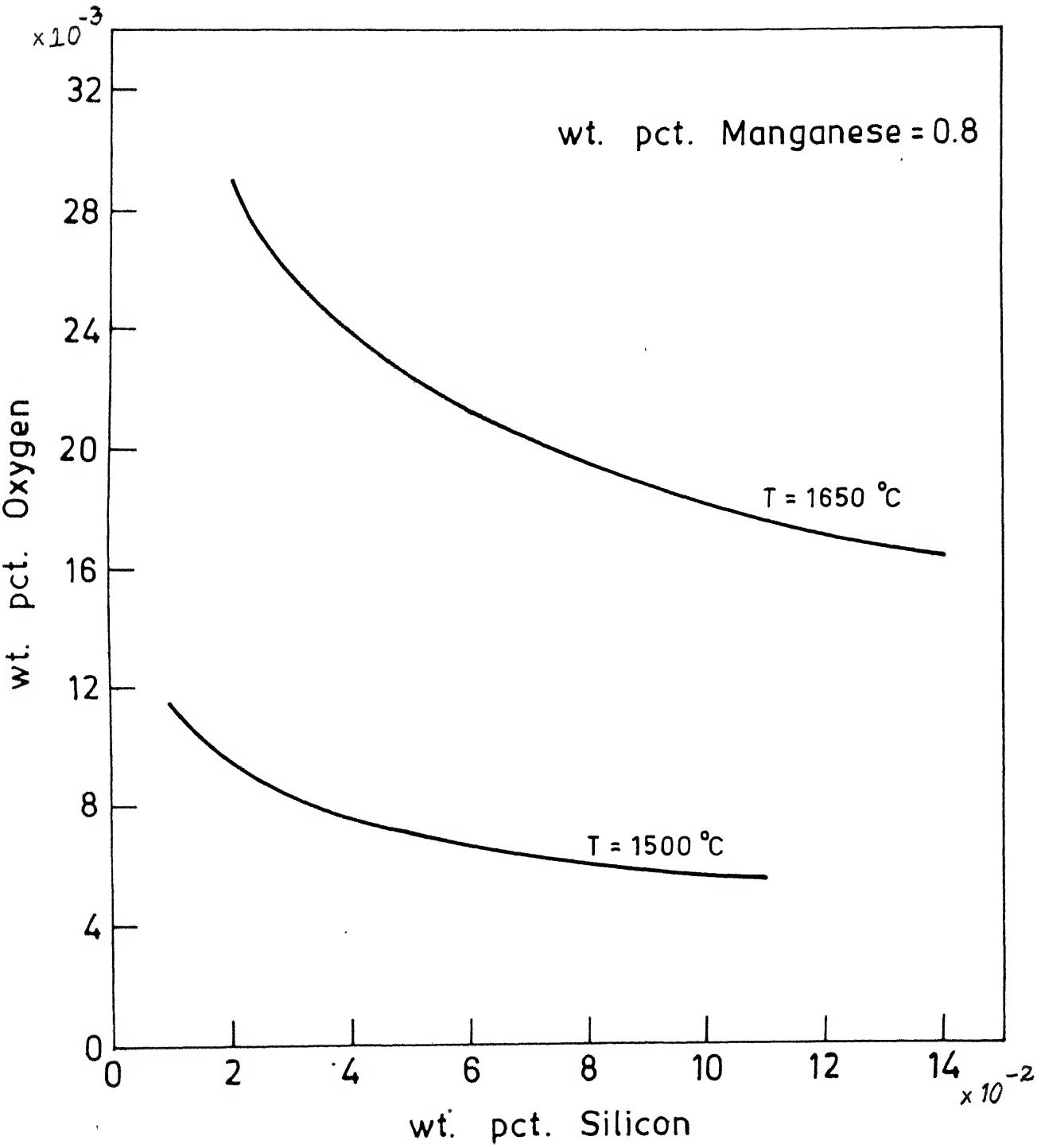

Fig. 18 Effect of temperature on Fe-Mn-Si-O equilibria.

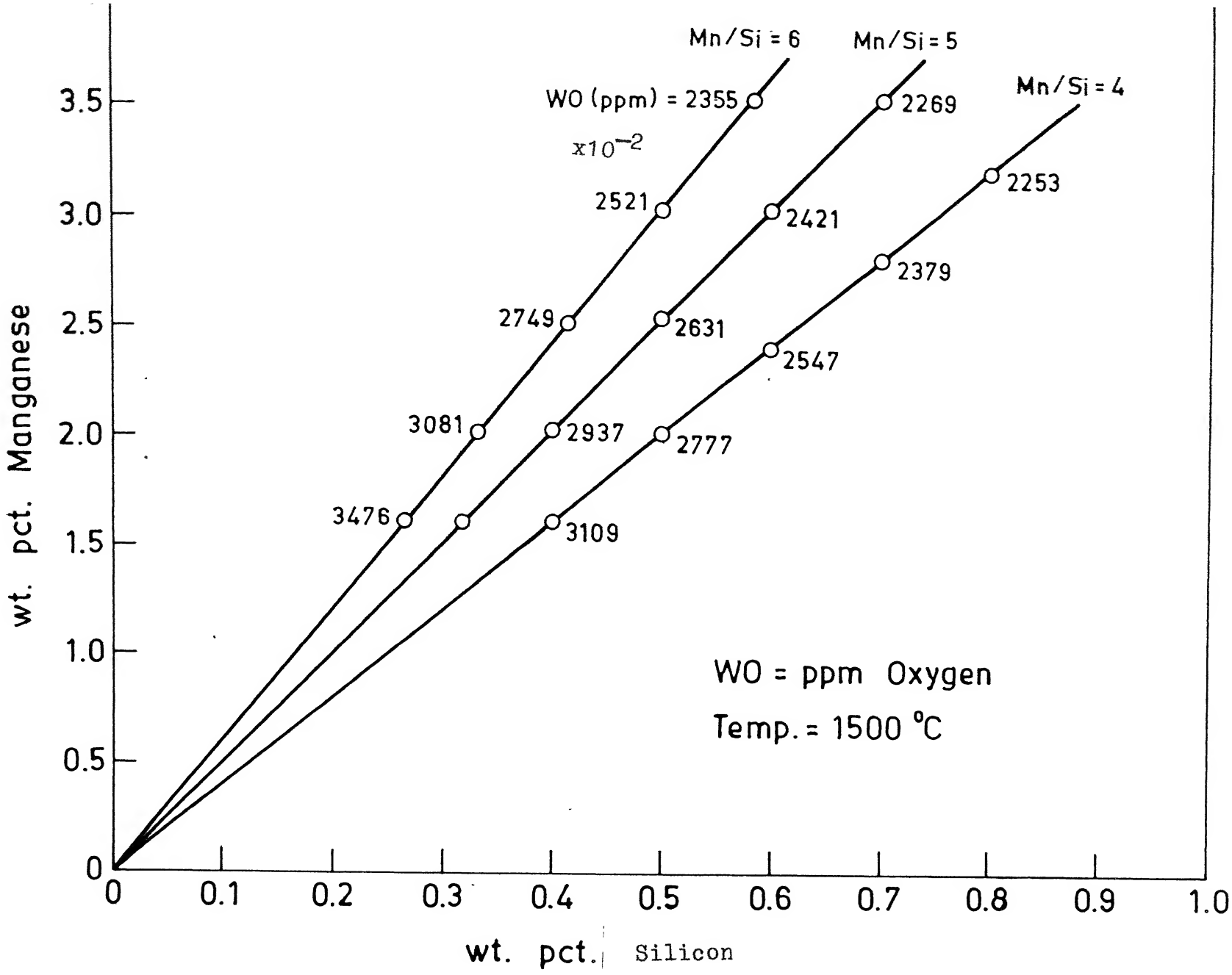
Mn/Si = 6
Mn/Si = 5
Mn/Si = 4
WO (ppm) = 2355
x10⁻²
2269
2253
2521
2421
2379
2749
2631
2547
3081
2937
2777
3476
3109
WO = ppm Oxygen
Temp. = 1500 °C
wt. pct. Manganese
wt. pct. Silicon
0
0.5
1.0
1.5
2.0
2.5
3.0
3.5
0.1
0.2
0.3
0.4
0.5
0.6
0.7
0.8
0.9
1.0

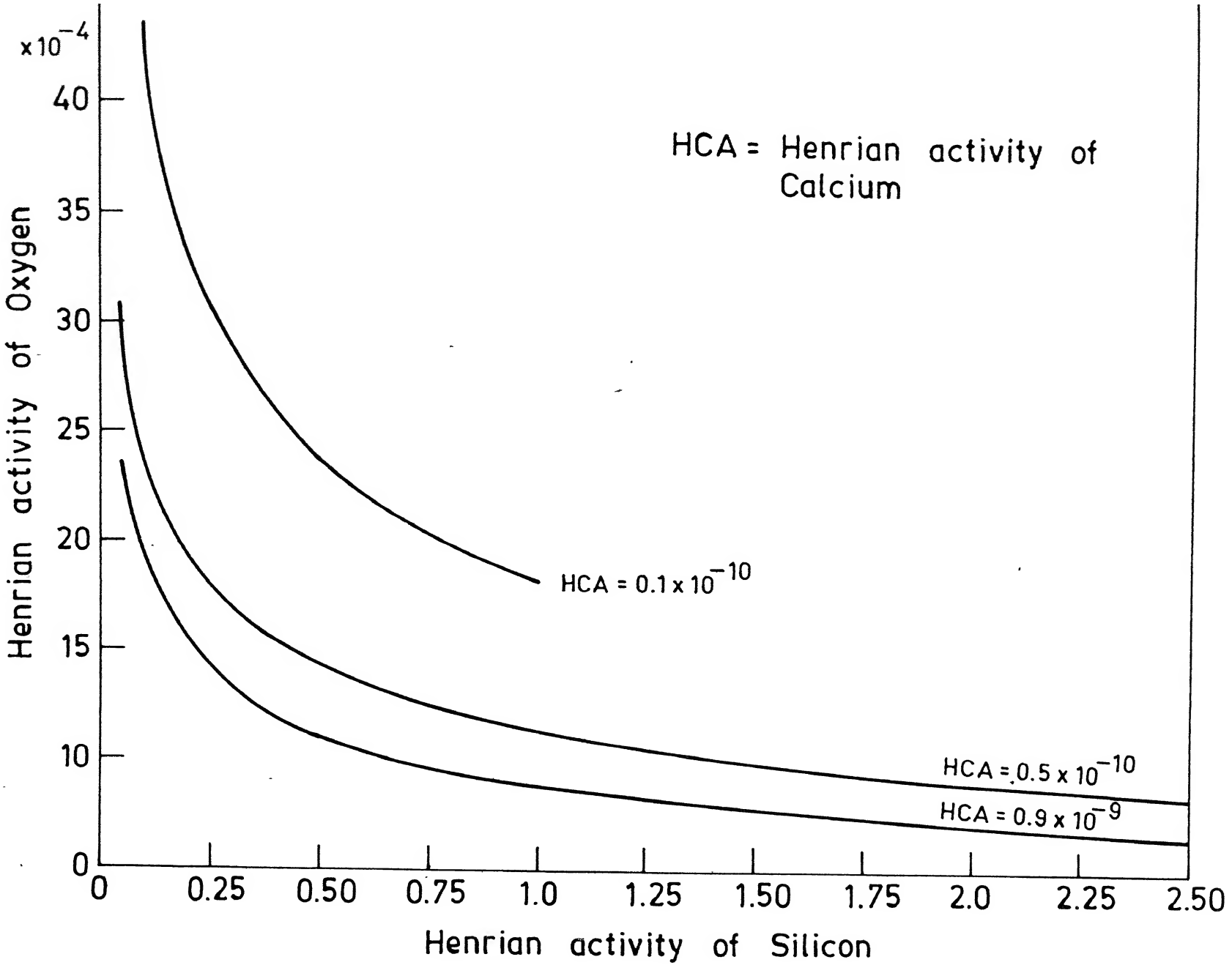
x10⁻⁴
40
35
30
25
20
15
10
0
Henrian activity of Oxygen
HCA = Henrian activity of Calcium
HCA = 0.1 x 10⁻¹⁰
HCA = 0.5 x 10⁻¹⁰
HCA = 0.9 x 10⁻⁹
0
0.25
0.50
0.75
1.0
1.25
1.50
1.75
2.0
2.25
2.50
Henrian activity of Silicon

experimental activity-composition data available in the literature. Mn-Al deoxidation involving MnO-Al_2O_3 slag, was carried out using the activity-composition diagram given by Jacob.[55] However, reproducibility of results in the regression analysis was poor due to the complex nature of their curves, hence this system was not solved. In the case of Si-Al deoxidation, the product slag is solid at all compositions and the thermodynamic models in the present study are not applicable.

(b) Complex deoxidation by Mn, Si and Ca involving complex FeO-M_xO_y-N_pO_q slags

The results of Mn-Si, Ca-Si and Ca-Mn deoxidation which give FeO-MnO-SiO_2, FeO-CaO-SiO_2 and CaO-MnO as the deoxidation product are compiled in Appendix 2. In each of the above cases graphical representation is not possible because for each set of activity values, unique values of equilibrium contents of oxygen and deoxidants exists. In the case of Ca-Si and Ca-Mn deoxidants, due to the limited number of activity data points available, only few scattered results are obtained. Work is being done on these systems to obtain analytical equations based on slag theories. In future this may enable one to calculate the equilibrium contents of the deoxidants and oxygen over the entire liquid range.

Si-Mn deoxidation involving FeO-MnO-SiO_2 slags was extensively studied in the present work. As discussed in Section 3.2.2, three different sets of activity composition phase diagrams are available (Table 9). In the present work, the data from all three sources was used and the corresponding

results obtained are compiled in Appendix 2. The limitation here is again the small number of data points obtained from the $FeO-MnO-SiO_2$, activity-composition diagrams. One may use analytical equations based on ideal silicate mixing or Regular solution model to obtain the activities of FeO, MnO and SiO_2. Due to the complexities of calculation involved in ideal silicate mixing equations, the analytical expressions based on regular solution model have been used in the present work. As explained in Section 3.2.2 the activity of FeO, MnO and SiO_2 are obtained from equations (3.2.6) to (3.2.8), for any fixed slag composition within the liquid range of the ternary phase diagram. At this stage it is difficult to justify which out of the four data sources compiled in Table 9 is the correct one to be chosen for the Mn-Si deoxidation involving $FeO-MnO-SiO_2$ slag. The thermodynamic model proposed for a study of this equilibria by Palmaers et al[38] was simulated using expressions based on regular solution model obtained in the present study in Section 3.2.2. It is found that the empirical relation given in equation (3.2.14) by Palmaers et al

$$a_{MnO} \times a_{SiO_2} = \text{Constant}$$

is not valid in the present study. This may be due to the fact that they employed the analytical expressions obtained by Scimar[26] for computer simulation of $FeO-MnO-SiO_2$ activity-composition diagram, incorporating a changed standard state of MnO (solid state instead of liquid).

CHAPTER 4

CONCLUSIONS

(1) Deoxidation equilibria in systems containing manganese, silicon, aluminium and calcium involving slag product of the types $FeO-M_xO_y$, $M_xO_y-N_pO_q$, $FeO-M_xO_y-N_pO_q$ (M, N = Mn, Si, Al, Ca) has been studied, using the activity-composition data of the respective slags through efficient computer oriented thermodynamic calculation models.

(2) The activity-composition data for the various slags involved, $FeO-M_xO_y$, $M_xO_y-N_pO_q$ and $FeO-M_xO_y-N_pO_q$ (M, N = Mn, Si, Al, Ca) has been reviewed.

(3) The formation of $FeO-M_xO_y$ type complex deoxidation product significantly influenced the equilibria compared to simple deoxidation with pure oxide as the slag. The equilibrium contents of the deoxidants decreases significantly in the presence of FeO in the slag.

(4) The increasing trend in the deoxidation powers as Ca-Al > Ca-Si > Si-Mn was established.

(5) For $FeO-M_xO_y-N_pO_q$ type deoxidation product the equilibrium contents of the oxygen and the deoxidants M and N (Si, Mn, Ca) were found for various slag compositions.

(6) In the case of Mn-Si deoxidation involving FeO-MnO-SiO_2 slags, analytical expression obtained from regular solution model were employed, to calculate the activities in the entire liquid range. These data were used to evaluate the equilibrium concentration of deoxidisers and the oxygen dissolved in liquid steel.

REFERENCES

1. H.E. McGannon (Ed.), "The Making, Shaping and Treating of Steel",Ed.9, U.S.S. Corporation, Pennsylvania, U.S.A., 1970, p.333.

2. R. Kiessling and N. Lange, "Non-Metallic Inclusions in Steel",The Metals Society, London, 1978, pp.11-15.

3. Proc."Clean Steel", Balatonfured, The Metals Society, London, 1983.

4. F.B. Pickering, "Inclusions", Institution of Metallurgists, London, 1979.

5. C. Bodsworth, "Physical Chemistry of Iron and Steel Manufacture", Ed. 1, ELBS and Longmans,Green and Co. Ltd., London, 1965, p. 365.

6. A.K. Bagaria, B.Tech. Thesis, I.I.T., Kanpur, 1977.

7. A. Ghosh, "Theory of Metallurgical Processes-Deoxidation and Pitside Practice", Summer School Notes, I.I.T., Kanpur, 1985. CF: G.V.R. Murthy, M.Tech. Thesis, I.I.T., Kanpur, 1984.

8. G.K. Sigworth and J.F. Elliott, Metal Science,8 (1974), 298.

9. D.L. Sponseller and R.A. Flinn, Trans. AIME, 230 (1964), 876.

10. S. Kobyashi, Y. Omori and K. Sanbongi, Trans. ISIJ, 11 (1971), 260.

11. G. Faulring and S. Ramalingam, Met. Trans. B, 11B (1980), 125.

12. S. Gustaffson and P.O. Mellberg, Proc.Symp,, Shangai, 1982.

13. W.A. Fischer and H.J. Fleischer, Arch.Eisen, 32 (1961), 1.

14. W.A. Fischer and P.W. Bardenheuer, Arch. Eisen, 39 (1968), 637.

15. K. Schwerdtfeger and A. Muan, Trans. AIME, 239 (1967), 1114.

16. E.T. Turkdogan, Proc. Symp., 'Application of Ferrous Metallurgy', 1971, Sheffield Univ., Iron and Steel Institute, London, 1973, p. 21.

17. R. Schuhuman, Jr. and P.J. Ensio, Trans. AIME, 191 (1951), 401.

18. E.J. Michal and R. Schuhuman Jr., Trans.AIME, 194 (1952), 723.

19. E.T. Turkdogan and J. Pearson, JISI, 173 (1953), 217.

20. C. Bodsworth, JISI, 193 (1959), 13.

21. J.F. Elliott, J. Metals, 7 (1955), 485.

22. S. Banya, A. Chiba and A. Hikosaka, Proc. Australia Japan Extractive Metallurgy Symposium, Sydney, Australia, 1980.

23. M. Iwase, N. Yamada, N. Nishida and E. Ichise, Trans. ISS, 4 (1984), 69.

24. H.B. Bell, A.B. Murad and P.T. Carter, J. Metals, 4 (1952), 718.

25. K.P. Abraham, M.W. Davies and F.D. Richardson, JISI, 196 (1960), 82.

26. R. Scimar, Rev. Univ. Mines, Ser. 9, 18 (1962), 602.

27. R.A. Walsch and S. Ramachandran, Trans. AIME, 227 (1963), 560.

28. H.B. Bell, JISI, 201 (1963), 116.

29. W.A. Fischer and P.W. Bardenheuer, Arch. Eisen., 39 (1968), 559.

30. N. Meysson and A. Rist, Rev. Met., ? 66 (1969), 115.

31. N.F. Grevillius, Jern. Ann., 153 (1969), 547; CF:
(i) F. Korber and W. Oelsen, Mitt. Kaiser-Wilhelm Inst. Eisen., 15 (1933), 271.
(ii) C.F. Herty and G.R. Fitterer, U.S. Bureau of Mines, Rep. No. 3081 (1931).

32. H. Fujita and S. Maruhashi, Tetsu-to-Hagane, 56 (1970), 830.

33. I.D. Sommerville, I. Ivanchev and H.B. Bell, Proc. Symp., "Application of Ferrous Production Metallurgy", 1971, Sheffield Univ., Iron and Steel Institute, London, 1973, p. 23.

34. A. Jacquemot and C. Gatellier, IRSID, RE 289, ECSC No. 6210-50 (1975).

35. Y. Wanibe, Y. Yamauchi, K. Kawai and H. Sakao, Arch. Eisen, 44 (1973), 711.

36. T. Fujisawa and H. Sakao, Tetsu-to-Hagane, 63 (1977), 72.

37. L. Blazenko Korousic, Radex Rudschau, (1980), 249.

38. A. Palmaers and P. Dauby, Proc. "Clean Steel", Balanton-fured, 1981, The Metals Society, London, (1983), p. 138.

39. B.K.D.P. Rao and D.R. Gaskell, Met. Trans. B, 12B (1981), 311.

40. W.J. Rankin, Met. Trans. B, 9B (1978), 726.

41. D.R. Gaskell, Met. Trans. B, 8B (1977), 131.

42. V.D. Eisenhuttenleute, "Slag Atlas", Verlag Stahleisen M.B.H., Dusseldorf, Germany, 1981.

43. E.T. Turkdogan, "Physicochemical Properties of Molten Slags and Glasses", The Metals Society, London, 1983, p. 89.

44. J.D. Baird and J. Taylor, Trans. Farad. Soc., 56 (1960), 1372.

45. D.A.R. Kay and J. Taylor, Trans. Farad. Soc., 56 (1960), 1372.

46. R.A. Sharma and F.D. Richardson, JISI, 200 (1962), 373.

47. M. Timucin and A.E. Morris, Met. Trans. AIME, 3 (1970), 3193.

48. M.L. Kapoor and M.G. Frohberg, Proc. Symp., "Application of Ferrous Metallurgy", 1971, Sheffield Univ., Iron and Steel Institute, London, 1973, p.17.

49. C.R. Masson, JISI, 210 (1972), 86.

50. Wanibe Yoshimoto, Y. Yamauchi, K. Kawai and H. Sakao, Arch. Eisen., 44 (1973), 711.

51. P.T. Carter and T.G. Macfarlane, JISI, 185 (1957), 54.

52. R.A. Sharma and F.D. Richardson, JISI, 200 (1962), 373.

53. M. Faulring and S. Ramalingam, Met. Trans. B, 11-B (1980), 125.

54. N. Tiberg and A. Muan, Met. Trans. B, 1 (1970), 435.

55. K.T. Jacob, Canad. Met. Quart., 20 (1981), 89.